Special issue: Research report

A diffusion tensor imaging tractography atlas for virtual in vivo dissections

Marco Catani[a,b,*] and Michel Thiebaut de Schotten[a,b,c]

[a]Natbrainlab, Section of Brain Maturation, Institute of Psychiatry, King's College London, London, UK
[b]Centre for Neuroimaging Sciences, Institute of Psychiatry, King's College London, London, UK
[c]CENIR – Centre de Neuroimagerie de Recherche, Hopital de la Salpetriere, 75651 Paris, France

ARTICLE INFO

ABSTRACT

Diffusion tensor imaging (DTI) tractography allows perform virtual dissections of white matter pathways in the living human brain. In 2002, Catani et al. published a method to reconstruct white matter pathways using a region of interest (ROI) approach. The method produced virtual representations of white matter tracts faithful to classical post-mortem descriptions but it required detailed a priori anatomical knowledge. Here, using the same approach, we provide a template to guide the delineation of ROIs for the reconstruction of the association, projection and commissural pathways of the living human brain. The template can be used for single case studies and case–control comparisons. An atlas of the 3D reconstructions of the single tracts is also provided as anatomical reference in the Montreal Neurological Institute (MNI) space.

1. Introduction

The possibility of performing virtual dissections of white matter tracts and visualizing pathways in the living human brain is one of the most promising applications of diffusion tensor imaging (DTI) tractography (Catani and Mesulam, 2008a, this issue; Catani, 2006). Current DTI tractography methods require the delineation of regions of interest (ROIs) as starting "seed points" for tracking (Jones, 2008, this issue). One approach for ROIs delineation is the automatic application of normalized cortical or subcortical masks to single brain data sets (see for example, Lawes et al., 2008). The use of cortical masks is of particular help when trying to reduce tractography analysis time and operator-dependent biases. But these methods perform poorly when applied to pathological brains (e.g., when the anatomy is distorted by the underlying pathological process) or when the experimenter aims at describing inter-individual variability in tract anatomy (e.g., studying differences in the cortical projections of an individual tract in the normal population). Also the use of cortical masks is prone to generate artefactual reconstructions of tracts due to high uncertainty of the fiber orientation in the cortical voxels or surrounding white matter (Jones, 2003; Jones, 2008, this issue). An alternative strategy is to define the ROIs manually. This approach may overcome some of the problems mentioned above and has been successfully used in several tractography studies (Conturo et al., 1999; Concha et al., 2005; Basser et al., 2000; Catani et al., 2002; Mori et al., 2000). One limiting step
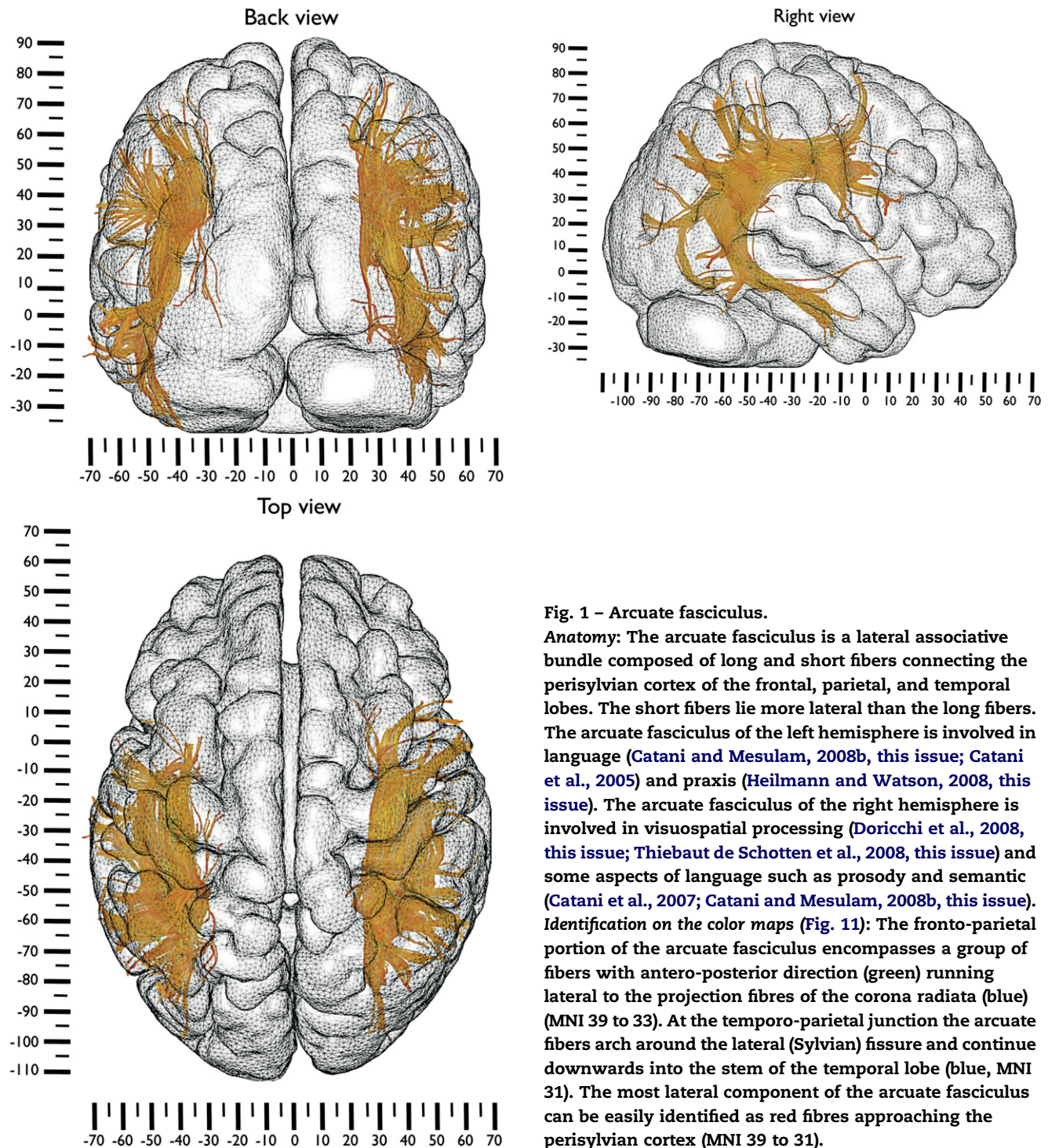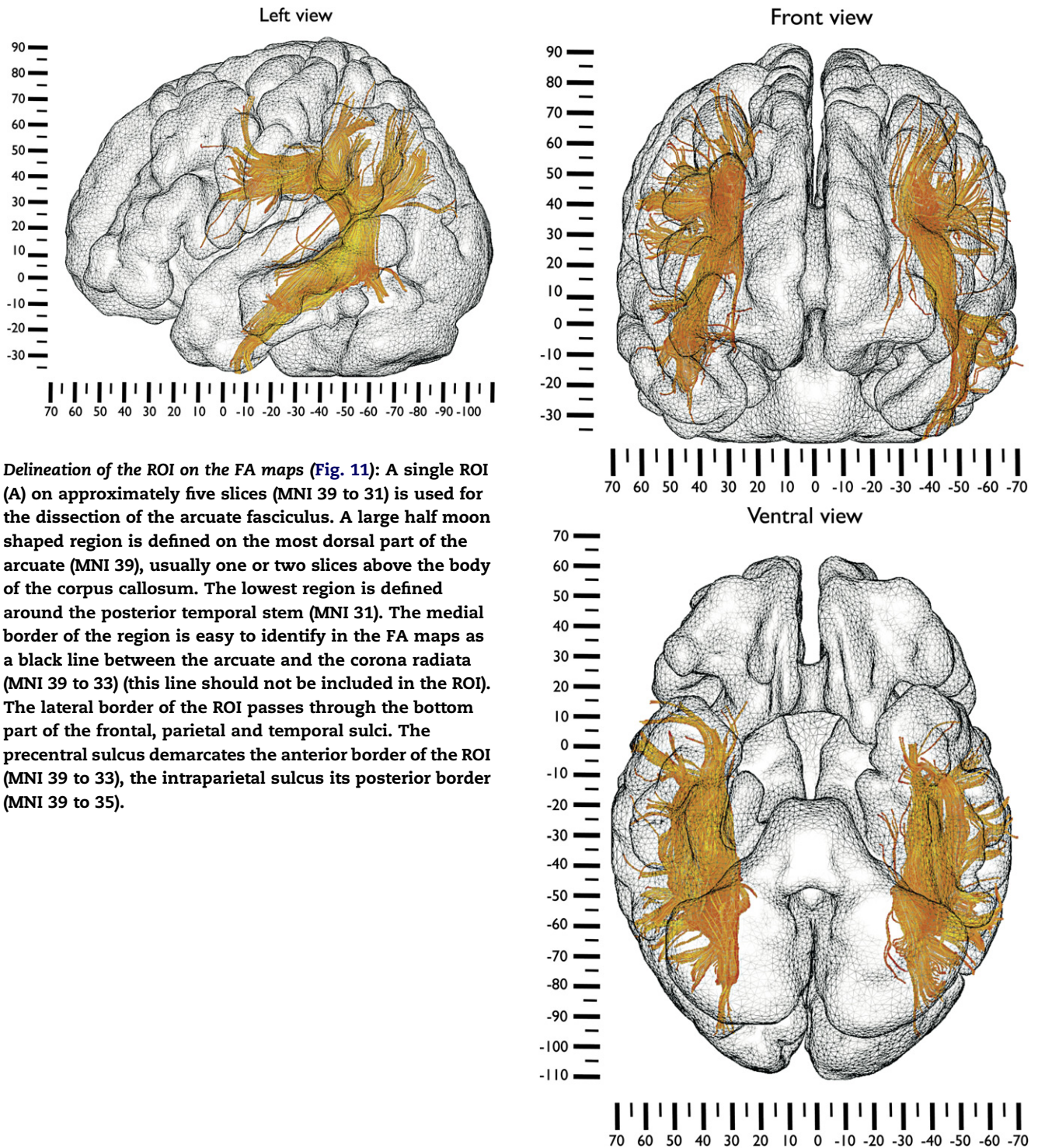
Back view

Right view

Top view

Fig. 1 – Arcuate fasciculus.

Anatomy: The arcuate fasciculus is a lateral associative bundle composed of long and short fibers connecting the perisylvian cortex of the frontal, parietal, and temporal lobes. The short fibers lie more lateral than the long fibers. The arcuate fasciculus of the left hemisphere is involved in language (Catani and Mesulam, 2008b, this issue; Catani et al., 2005) and praxis (Heilmann and Watson, 2008, this issue). The arcuate fasciculus of the right hemisphere is involved in visuospatial processing (Doricchi et al., 2008, this issue; Thiebaut de Schotten et al., 2008, this issue) and some aspects of language such as prosody and semantic (Catani et al., 2007; Catani and Mesulam, 2008b, this issue). *Identification on the color maps* (Fig. 11): The fronto-parietal portion of the arcuate fasciculus encompasses a group of fibers with antero-posterior direction (green) running lateral to the projection fibres of the corona radiata (blue) (MNI 39 to 33). At the temporo-parietal junction the arcuate fibers arch around the lateral (Sylvian) fissure and continue downwards into the stem of the temporal lobe (blue, MNI 31). The most lateral component of the arcuate fasciculus can be easily identified as red fibres approaching the perisylvian cortex (MNI 39 to 31).

Left view

Front view

Ventral view

Delineation of the ROI on the FA maps ([Fig. 11](#)): A single ROI (A) on approximately five slices (MNI 39 to 31) is used for the dissection of the arcuate fasciculus. A large half moon shaped region is defined on the most dorsal part of the arcuate (MNI 39), usually one or two slices above the body of the corpus callosum. The lowest region is defined around the posterior temporal stem (MNI 31). The medial border of the region is easy to identify in the FA maps as a black line between the arcuate and the corona radiata (MNI 39 to 33) (this line should not be included in the ROI). The lateral border of the ROI passes through the bottom part of the frontal, parietal and temporal sulci. The precentral sulcus demarcates the anterior border of the ROI (MNI 39 to 33), the intraparietal sulcus its posterior border (MNI 39 to 35).
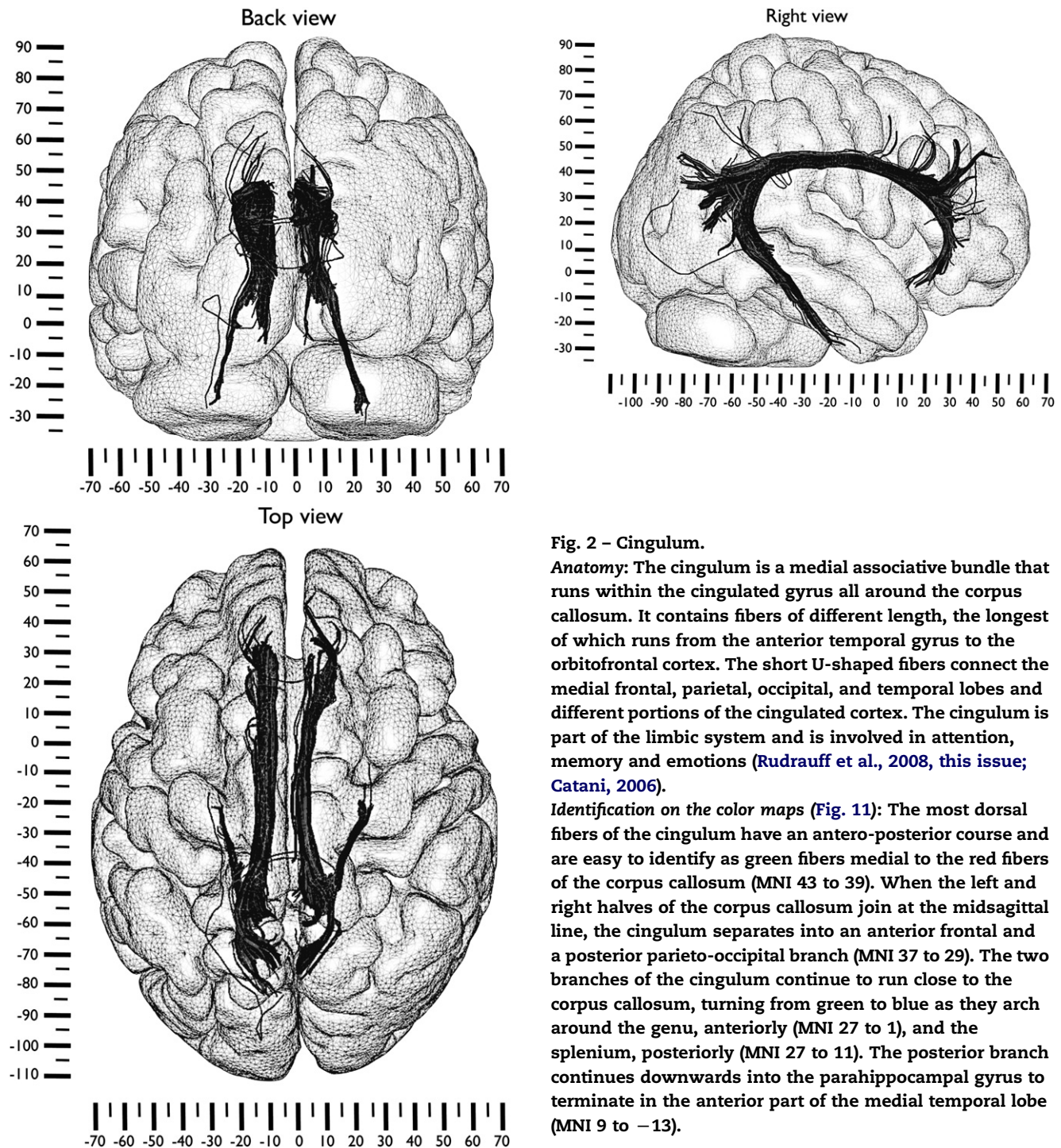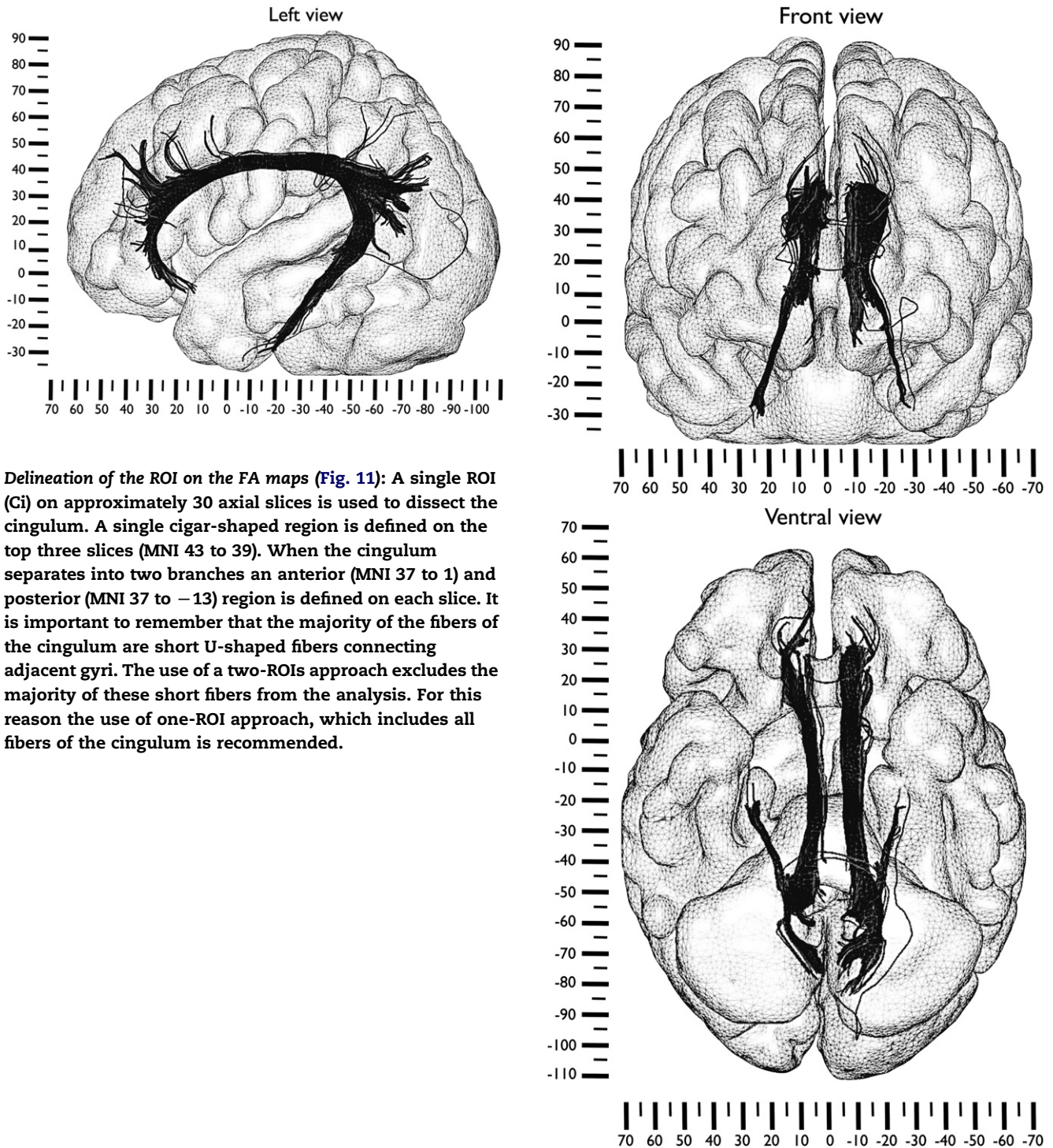
Fig. 2 – Cingulum.

Anatomy: The cingulum is a medial associative bundle that runs within the cingulated gyrus all around the corpus callosum. It contains fibers of different length, the longest of which runs from the anterior temporal gyrus to the orbitofrontal cortex. The short U-shaped fibers connect the medial frontal, parietal, occipital, and temporal lobes and different portions of the cingulated cortex. The cingulum is part of the limbic system and is involved in attention, memory and emotions (Rudrauff et al., 2008, this issue; Catani, 2006).

Identification on the color maps (Fig. 11): The most dorsal fibers of the cingulum have an antero-posterior course and are easy to identify as green fibers medial to the red fibers of the corpus callosum (MNI 43 to 39). When the left and right halves of the corpus callosum join at the midsagittal line, the cingulum separates into an anterior frontal and a posterior parieto-occipital branch (MNI 37 to 29). The two branches of the cingulum continue to run close to the corpus callosum, turning from green to blue as they arch around the genu, anteriorly (MNI 27 to 1), and the splenium, posteriorly (MNI 27 to 11). The posterior branch continues downwards into the parahippocampal gyrus to terminate in the anterior part of the medial temporal lobe (MNI 9 to −13).
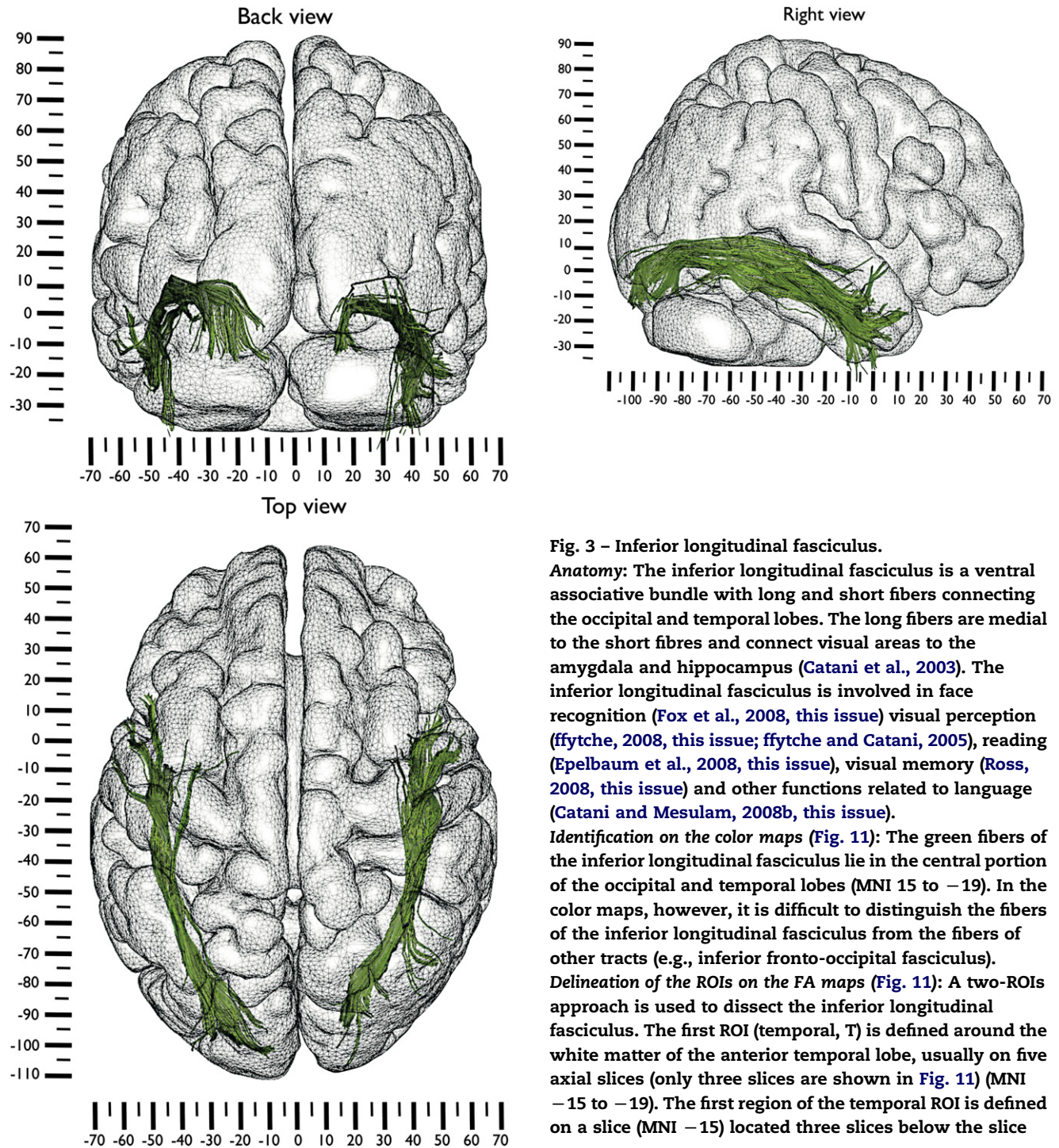
Left view

Front view

Ventral view

Delineation of the ROI on the FA maps (Fig. 11): A single ROI (Ci) on approximately 30 axial slices is used to dissect the cingulum. A single cigar-shaped region is defined on the top three slices (MNI 43 to 39). When the cingulum separates into two branches an anterior (MNI 37 to 1) and posterior (MNI 37 to −13) region is defined on each slice. It is important to remember that the majority of the fibers of the cingulum are short U-shaped fibers connecting adjacent gyri. The use of a two-ROIs approach excludes the majority of these short fibers from the analysis. For this reason the use of one-ROI approach, which includes all fibers of the cingulum is recommended.

Back view

Right view

Top view

Fig. 3 – Inferior longitudinal fasciculus.
Anatomy: The inferior longitudinal fasciculus is a ventral associative bundle with long and short fibers connecting the occipital and temporal lobes. The long fibers are medial to the short fibres and connect visual areas to the amygdala and hippocampus (Catani et al., 2003). The inferior longitudinal fasciculus is involved in face recognition (Fox et al., 2008, this issue) visual perception (ffytche, 2008, this issue; ffytche and Catani, 2005), reading (Epelbaum et al., 2008, this issue), visual memory (Ross, 2008, this issue) and other functions related to language (Catani and Mesulam, 2008b, this issue).
Identification on the color maps (Fig. 11): The green fibers of the inferior longitudinal fasciculus lie in the central portion of the occipital and temporal lobes (MNI 15 to −19). In the color maps, however, it is difficult to distinguish the fibers of the inferior longitudinal fasciculus from the fibers of other tracts (e.g., inferior fronto-occipital fasciculus).
Delineation of the ROIs on the FA maps (Fig. 11): A two-ROIs approach is used to dissect the inferior longitudinal fasciculus. The first ROI (temporal, T) is defined around the white matter of the anterior temporal lobe, usually on five axial slices (only three slices are shown in Fig. 11) (MNI −15 to −19). The first region of the temporal ROI is defined on a slice (MNI −15) located three slices below the slice
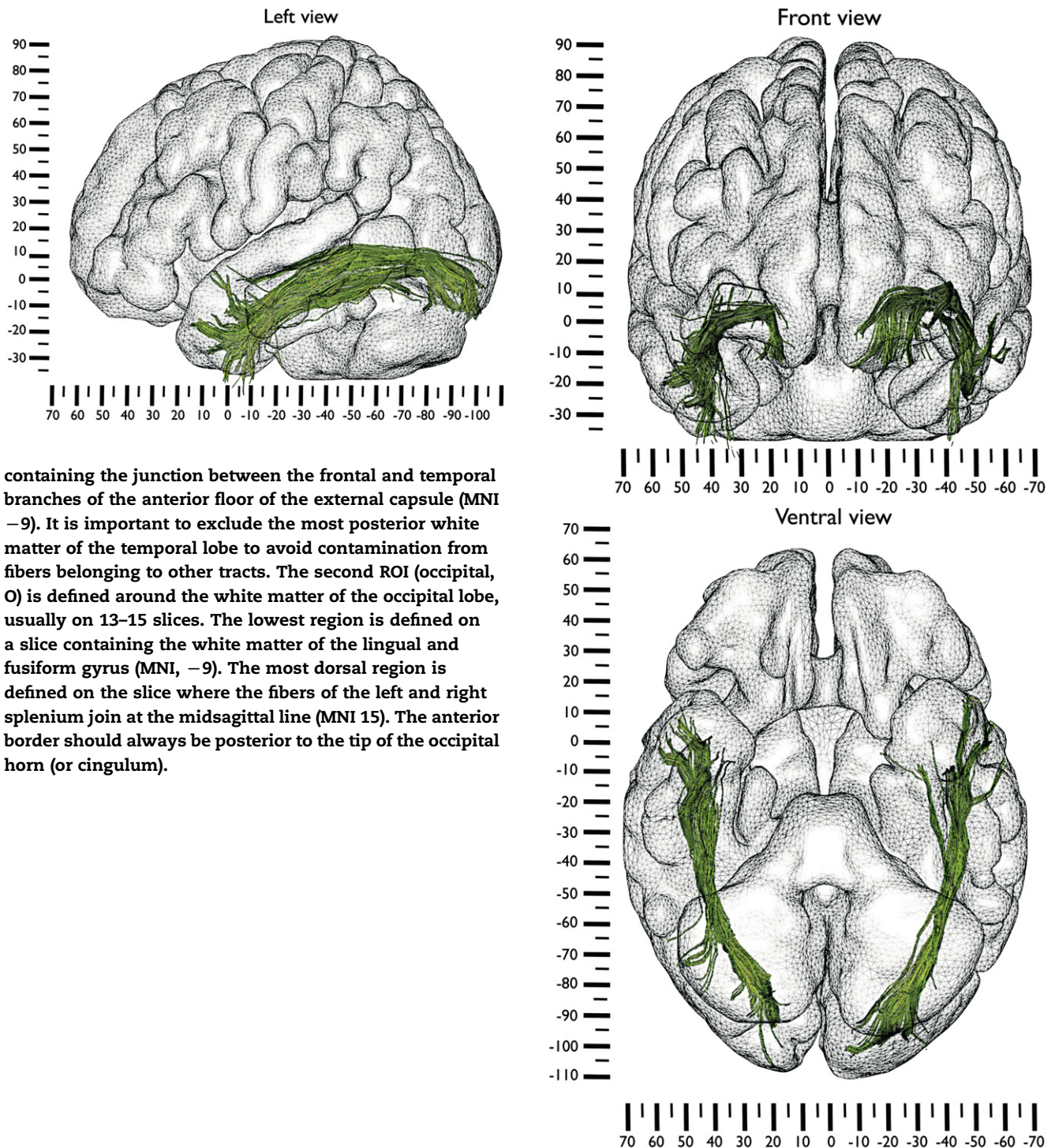
containing the junction between the frontal and temporal branches of the anterior floor of the external capsule (MNI −9). It is important to exclude the most posterior white matter of the temporal lobe to avoid contamination from fibers belonging to other tracts. The second ROI (occipital, O) is defined around the white matter of the occipital lobe, usually on 13–15 slices. The lowest region is defined on a slice containing the white matter of the lingual and fusiform gyrus (MNI, −9). The most dorsal region is defined on the slice where the fibers of the left and right splenium join at the midsagittal line (MNI 15). The anterior border should always be posterior to the tip of the occipital horn (or cingulum).
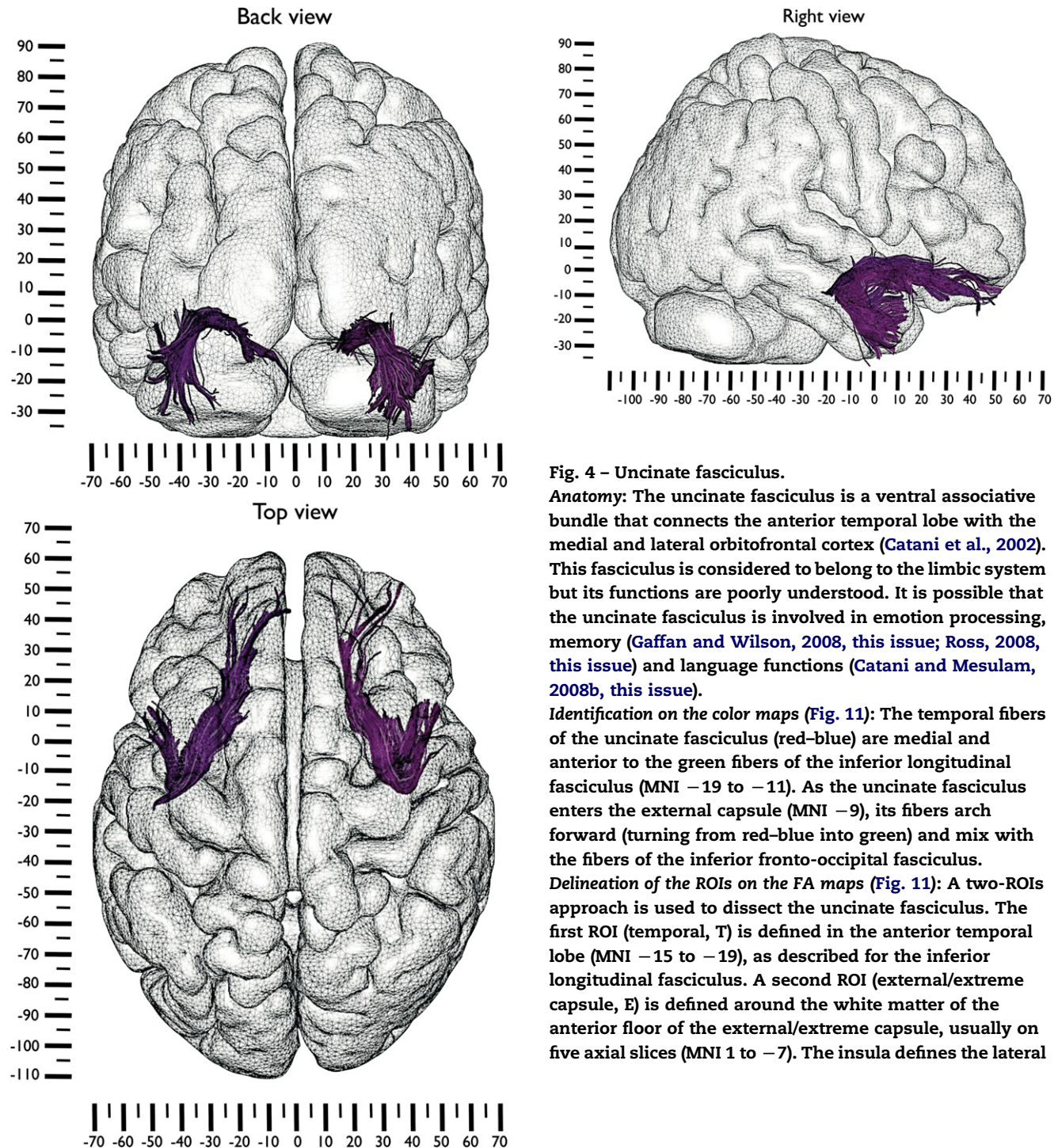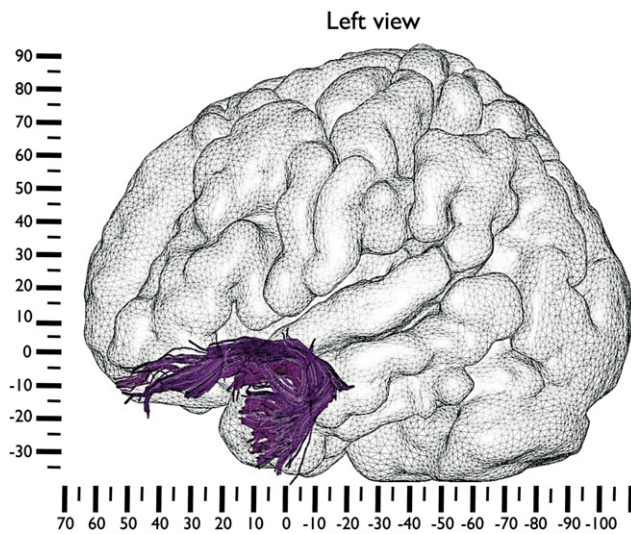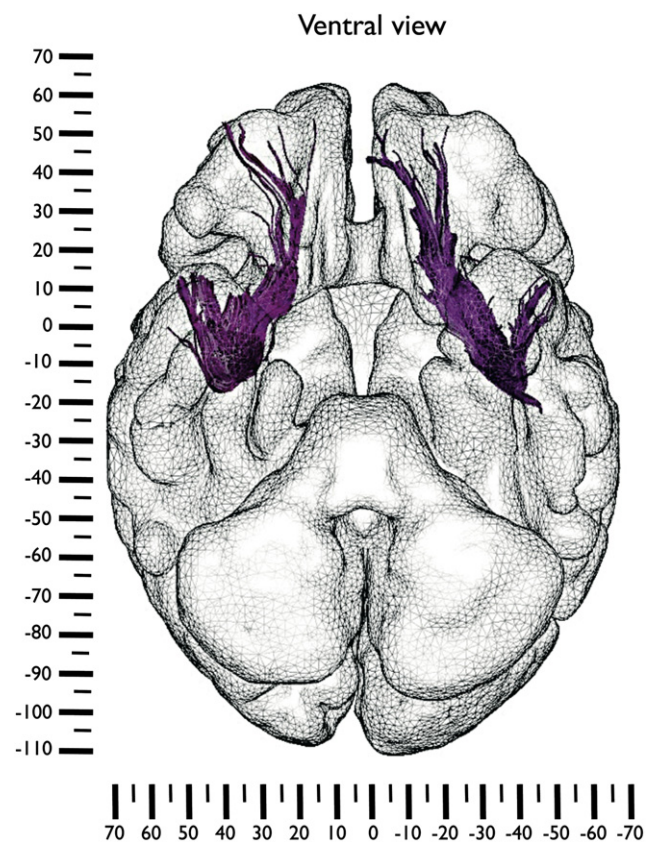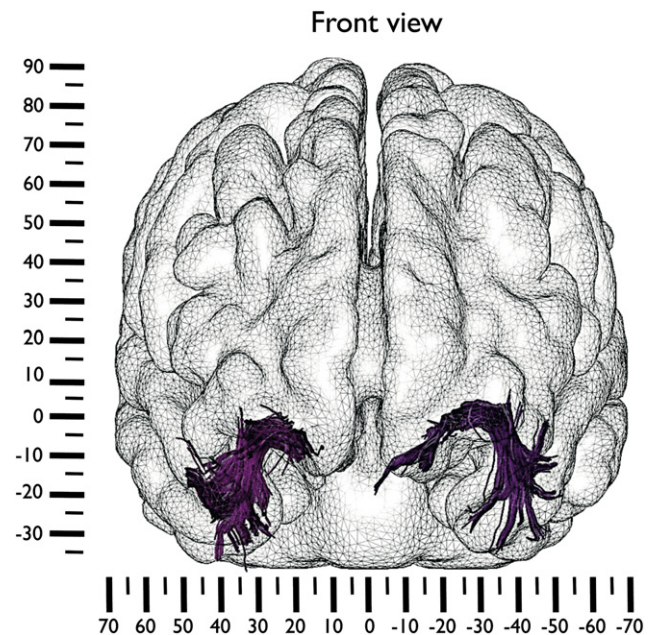
Fig. 4 – Uncinate fasciculus.

Anatomy: The uncinate fasciculus is a ventral associative bundle that connects the anterior temporal lobe with the medial and lateral orbitofrontal cortex (Catani et al., 2002). This fasciculus is considered to belong to the limbic system but its functions are poorly understood. It is possible that the uncinate fasciculus is involved in emotion processing, memory (Gaffan and Wilson, 2008, this issue; Ross, 2008, this issue) and language functions (Catani and Mesulam, 2008b, this issue).

Identification on the color maps (Fig. 11): The temporal fibers of the uncinate fasciculus (red–blue) are medial and anterior to the green fibers of the inferior longitudinal fasciculus (MNI −19 to −11). As the uncinate fasciculus enters the external capsule (MNI −9), its fibers arch forward (turning from red–blue into green) and mix with the fibers of the inferior fronto-occipital fasciculus.

Delineation of the ROIs on the FA maps (Fig. 11): A two-ROIs approach is used to dissect the uncinate fasciculus. The first ROI (temporal, T) is defined in the anterior temporal lobe (MNI −15 to −19), as described for the inferior longitudinal fasciculus. A second ROI (external/extreme capsule, E) is defined around the white matter of the anterior floor of the external/extreme capsule, usually on five axial slices (MNI 1 to −7). The insula defines the lateral

Left view

Front view

Ventral view

border of the ROI, the lenticular nucleus its medial border. We suggest beginning the delineation of this second ROI from the slice where the temporal and frontal branches of the external/extreme capsule join together (MNI −7). From here one can continue to move up to define the remaining four regions.
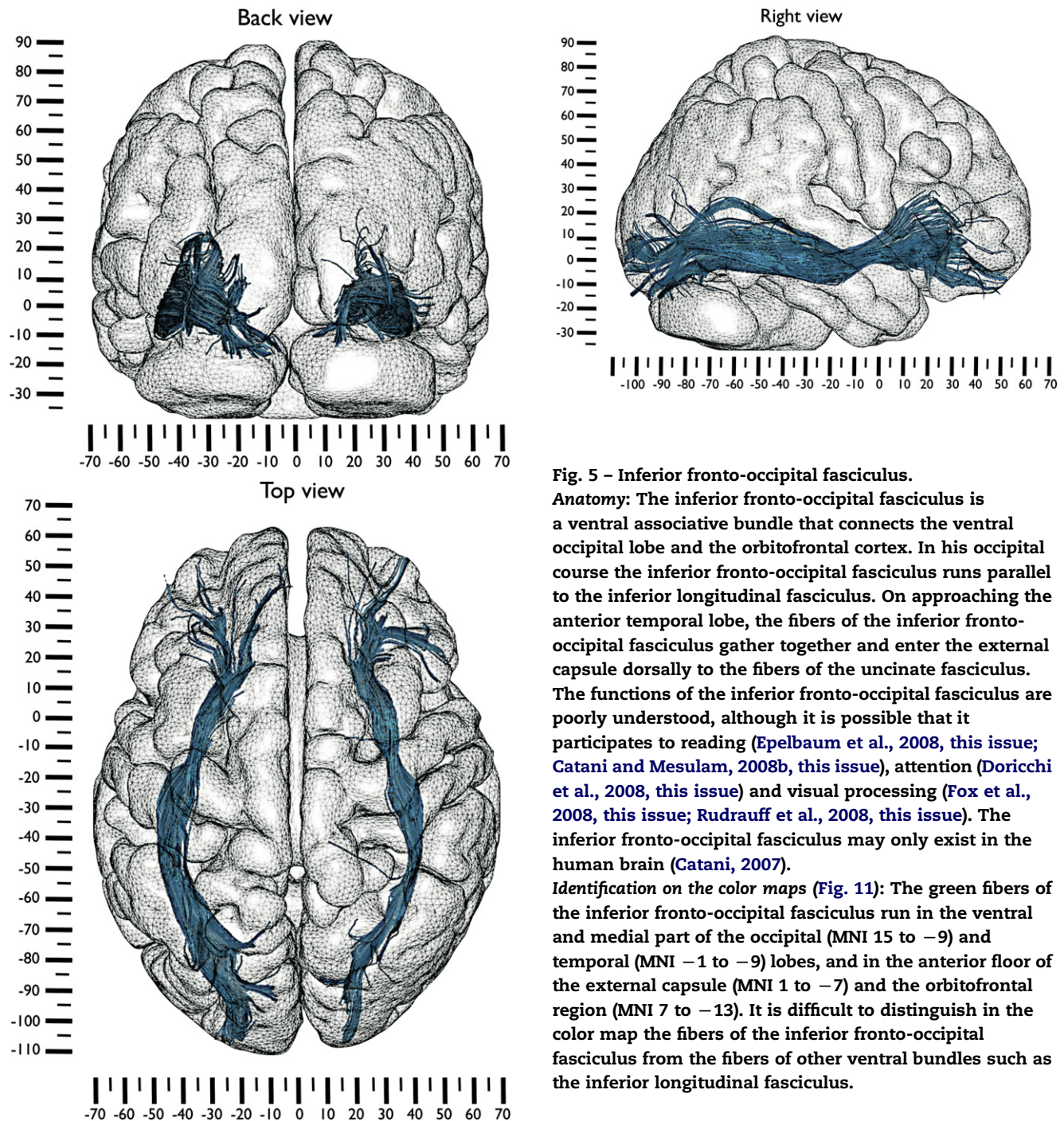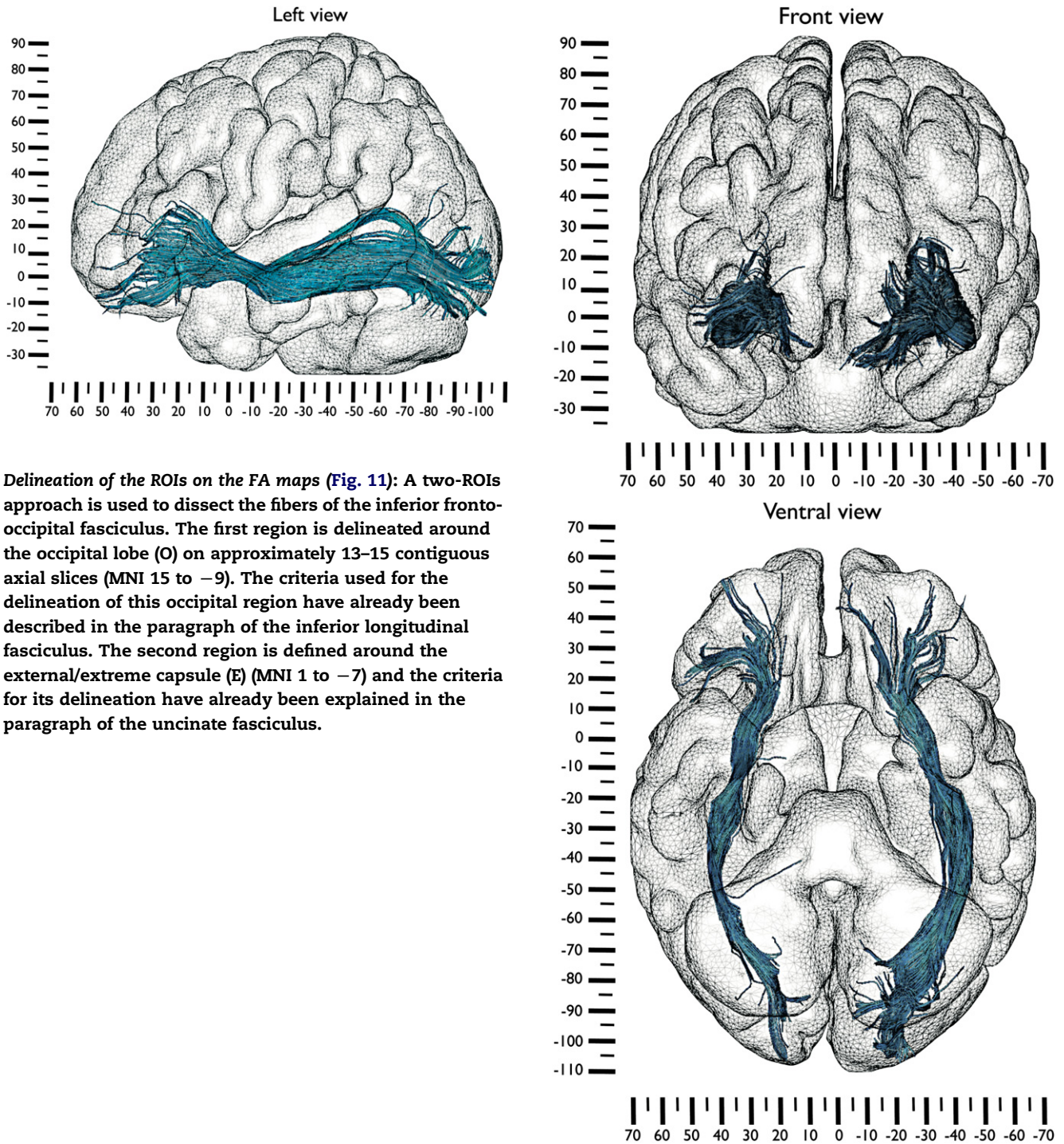
Back view

Right view

Top view

Fig. 5 – Inferior fronto-occipital fasciculus.
Anatomy: The inferior fronto-occipital fasciculus is a ventral associative bundle that connects the ventral occipital lobe and the orbitofrontal cortex. In his occipital course the inferior fronto-occipital fasciculus runs parallel to the inferior longitudinal fasciculus. On approaching the anterior temporal lobe, the fibers of the inferior fronto-occipital fasciculus gather together and enter the external capsule dorsally to the fibers of the uncinate fasciculus. The functions of the inferior fronto-occipital fasciculus are poorly understood, although it is possible that it participates to reading (Epelbaum et al., 2008, this issue; Catani and Mesulam, 2008b, this issue), attention (Doricchi et al., 2008, this issue) and visual processing (Fox et al., 2008, this issue; Rudrauff et al., 2008, this issue). The inferior fronto-occipital fasciculus may only exist in the human brain (Catani, 2007).
Identification on the color maps (Fig. 11): The green fibers of the inferior fronto-occipital fasciculus run in the ventral and medial part of the occipital (MNI 15 to −9) and temporal (MNI −1 to −9) lobes, and in the anterior floor of the external capsule (MNI 1 to −7) and the orbitofrontal region (MNI 7 to −13). It is difficult to distinguish in the color map the fibers of the inferior fronto-occipital fasciculus from the fibers of other ventral bundles such as the inferior longitudinal fasciculus.

Left view

Front view

Ventral view

Delineation of the ROIs on the FA maps (Fig. 11): A two-ROIs approach is used to dissect the fibers of the inferior fronto-occipital fasciculus. The first region is delineated around the occipital lobe (O) on approximately 13–15 contiguous axial slices (MNI 15 to −9). The criteria used for the delineation of this occipital region have already been described in the paragraph of the inferior longitudinal fasciculus. The second region is defined around the external/extreme capsule (E) (MNI 1 to −7) and the criteria for its delineation have already been explained in the paragraph of the uncinate fasciculus.
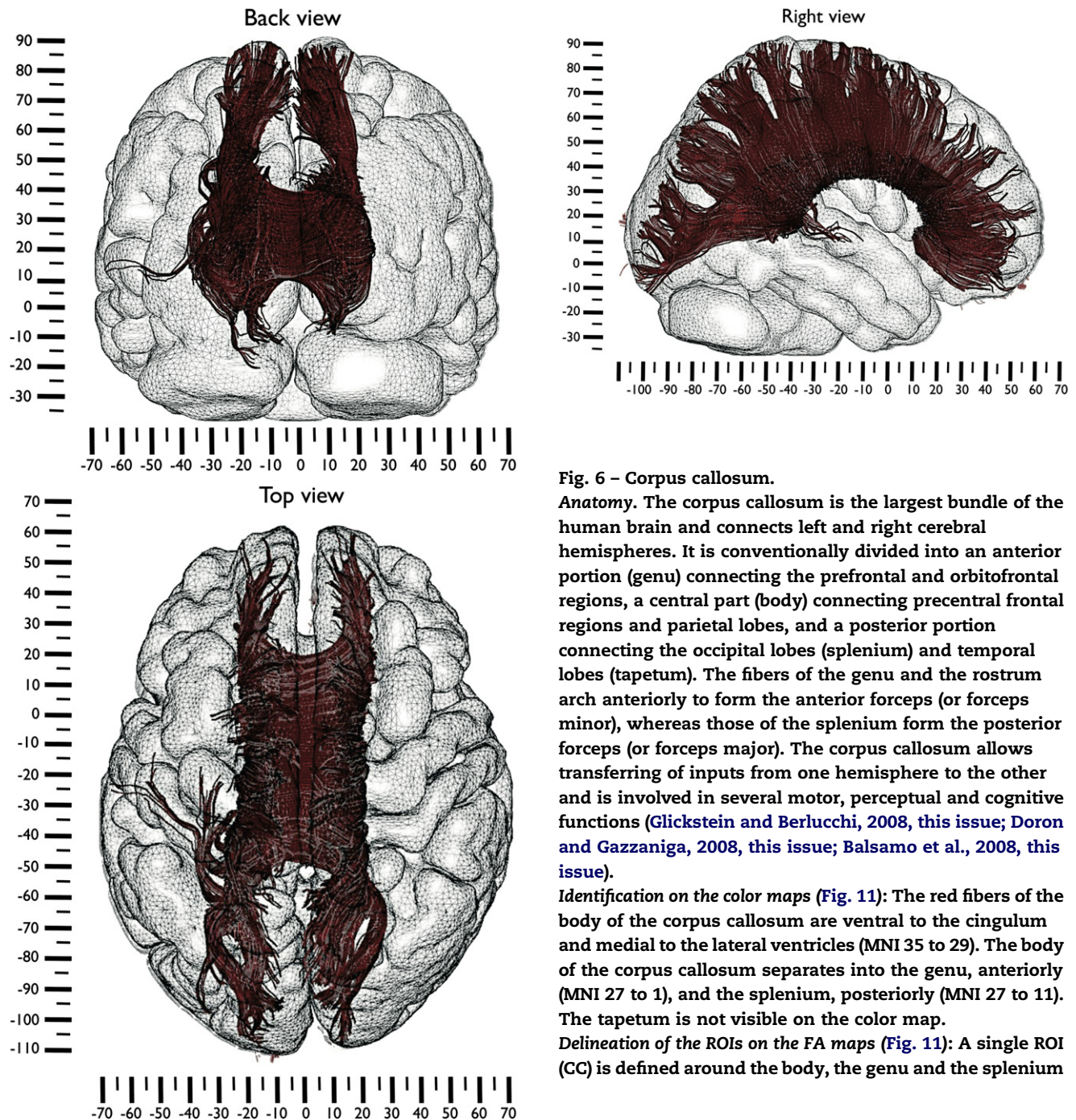
Back view

Right view


Top view

Fig. 6 – Corpus callosum.

Anatomy. The corpus callosum is the largest bundle of the human brain and connects left and right cerebral hemispheres. It is conventionally divided into an anterior portion (genu) connecting the prefrontal and orbitofrontal regions, a central part (body) connecting precentral frontal regions and parietal lobes, and a posterior portion connecting the occipital lobes (splenium) and temporal lobes (tapetum). The fibers of the genu and the rostrum arch anteriorly to form the anterior forceps (or forceps minor), whereas those of the splenium form the posterior forceps (or forceps major). The corpus callosum allows transferring of inputs from one hemisphere to the other and is involved in several motor, perceptual and cognitive functions (Glickstein and Berlucchi, 2008, this issue; Doron and Gazzaniga, 2008, this issue; Balsamo et al., 2008, this issue).

Identification on the color maps (Fig. 11): The red fibers of the body of the corpus callosum are ventral to the cingulum and medial to the lateral ventricles (MNI 35 to 29). The body of the corpus callosum separates into the genu, anteriorly (MNI 27 to 1), and the splenium, posteriorly (MNI 27 to 11). The tapetum is not visible on the color map.

Delineation of the ROIs on the FA maps (Fig. 11): A single ROI (CC) is defined around the body, the genu and the splenium

Left view

Front view

Ventral view
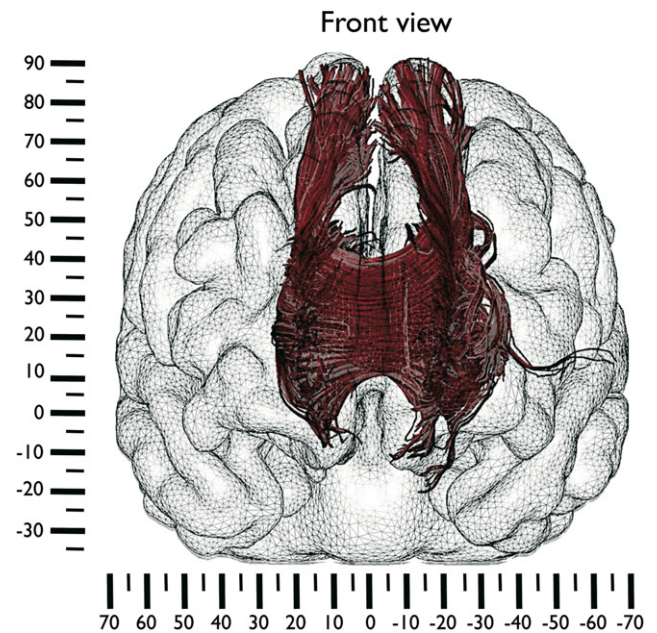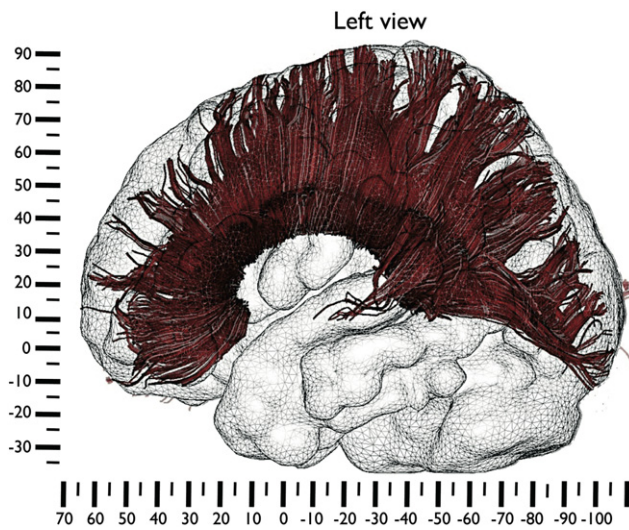
of the corpus callosum (MNI 35 to 5). The shape of the regions follows the anatomy of the different parts of the corpus callosum, butterfly-shaped for the body, horseshoe-shaped for genu and splenium. Alternatively, a single ROI defined around the corpus callosum on a midsagittal slice can be used (not shown).
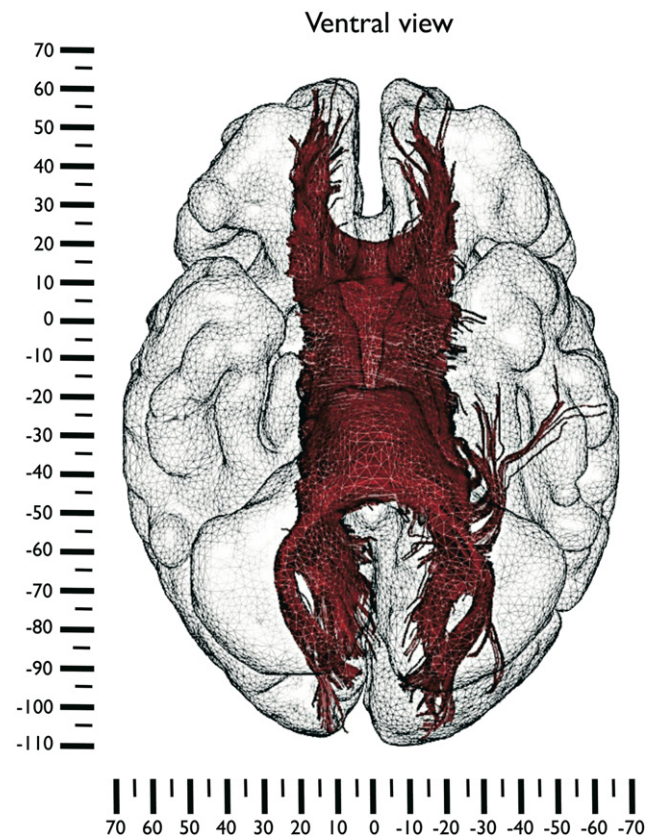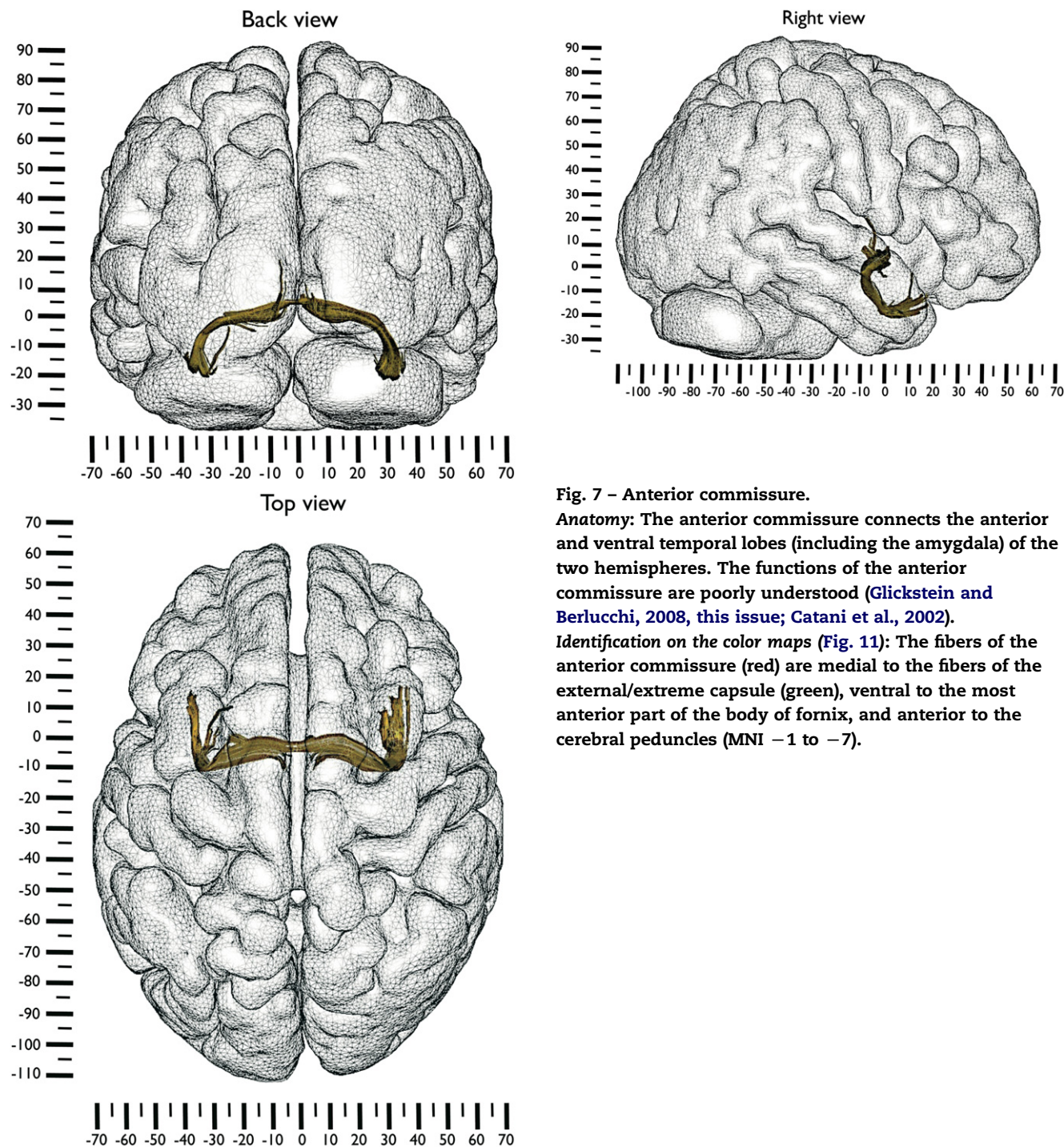
Fig. 7 – Anterior commissure.
Anatomy: The anterior commissure connects the anterior and ventral temporal lobes (including the amygdala) of the two hemispheres. The functions of the anterior commissure are poorly understood (Glickstein and Berlucchi, 2008, this issue; Catani et al., 2002).
Identification on the color maps (Fig. 11): The fibers of the anterior commissure (red) are medial to the fibers of the external/extreme capsule (green), ventral to the most anterior part of the body of fornix, and anterior to the cerebral peduncles (MNI −1 to −7).

Left view

Front view

Ventral view

Delineation of the ROI on the FA maps (Fig. 11): A one-ROI approach is used to dissect the anterior commissure. The ROI (AC) is defined around the lateral branches of the anterior commissure on four axial slices (MNI −1 to −7). To avoid contamination from the fibers of the uncinate and inferior fronto-occipital fasciculus, the most lateral fibers of the anterior commissure, which are close to the external capsule, should be excluded from the region (MNI −7).

Back view

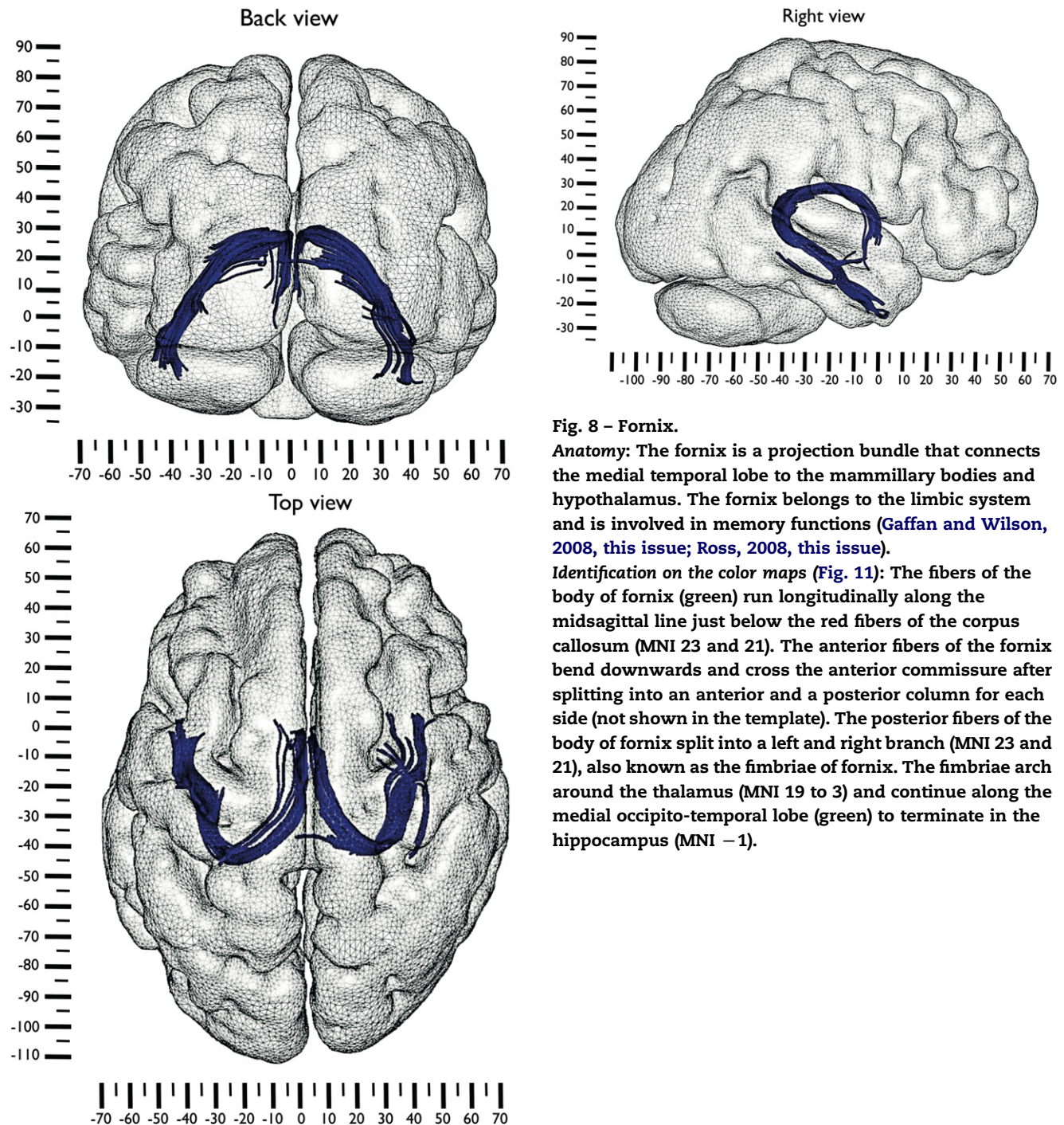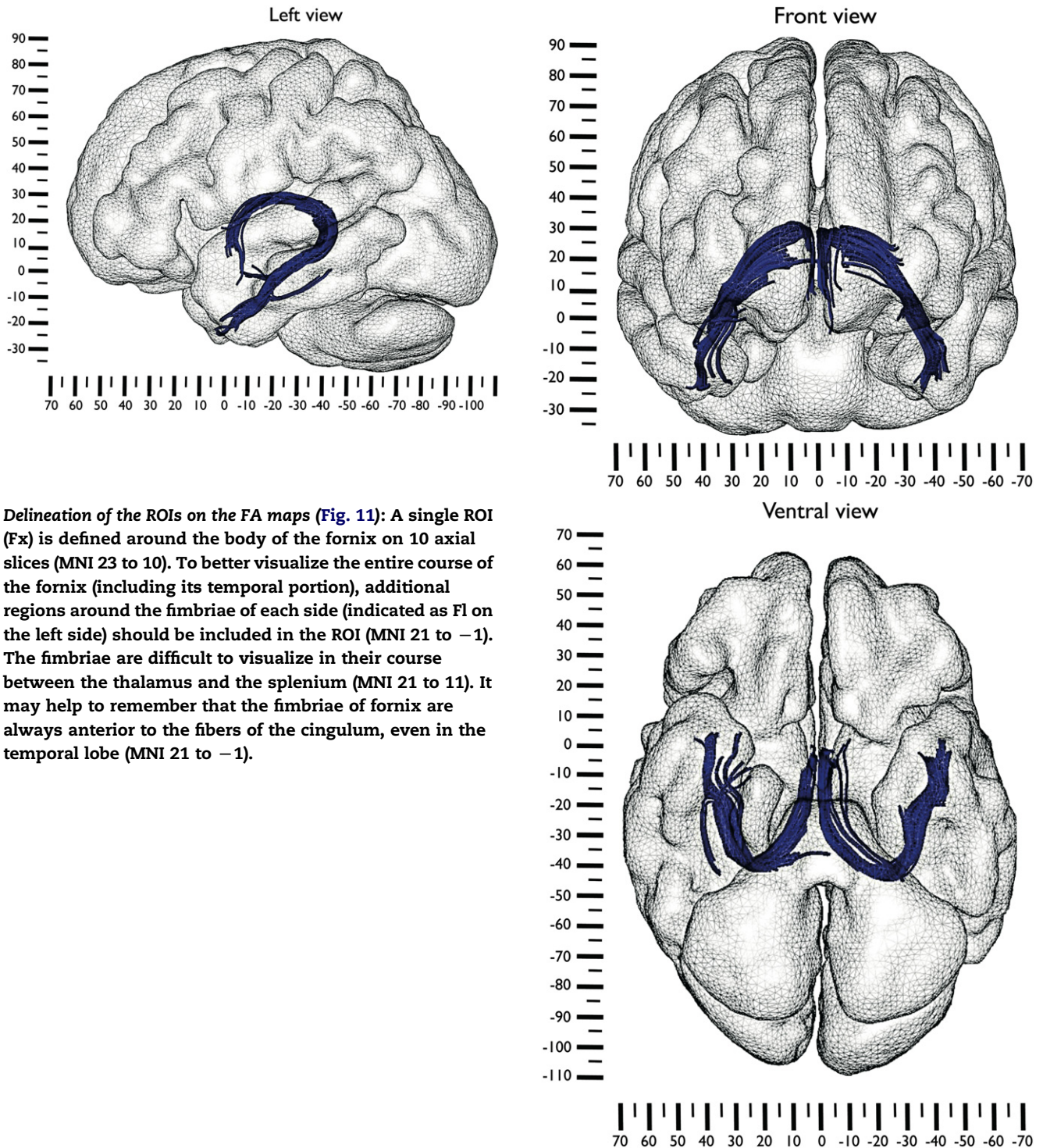## Right view

Top view

Fig. 8 – Fornix.

Anatomy: The fornix is a projection bundle that connects the medial temporal lobe to the mammillary bodies and hypothalamus. The fornix belongs to the limbic system and is involved in memory functions (Gaffan and Wilson, 2008, this issue; Ross, 2008, this issue).

Identification on the color maps (Fig. 11): The fibers of the body of fornix (green) run longitudinally along the midsagittal line just below the red fibers of the corpus callosum (MNI 23 and 21). The anterior fibers of the fornix bend downwards and cross the anterior commissure after splitting into an anterior and a posterior column for each side (not shown in the template). The posterior fibers of the body of fornix split into a left and right branch (MNI 23 and 21), also known as the fimbriae of fornix. The fimbriae arch around the thalamus (MNI 19 to 3) and continue along the medial occipito-temporal lobe (green) to terminate in the hippocampus (MNI −1).

Left view

Front view

Ventral view

Delineation of the ROIs on the FA maps (Fig. 11)**: A single ROI (Fx) is defined around the body of the fornix on 10 axial slices (MNI 23 to 10). To better visualize the entire course of the fornix (including its temporal portion), additional regions around the fimbriae of each side (indicated as Fl on the left side) should be included in the ROI (MNI 21 to −1). The fimbriae are difficult to visualize in their course between the thalamus and the splenium (MNI 21 to 11). It may help to remember that the fimbriae of fornix are always anterior to the fibers of the cingulum, even in the temporal lobe (MNI 21 to −1).**
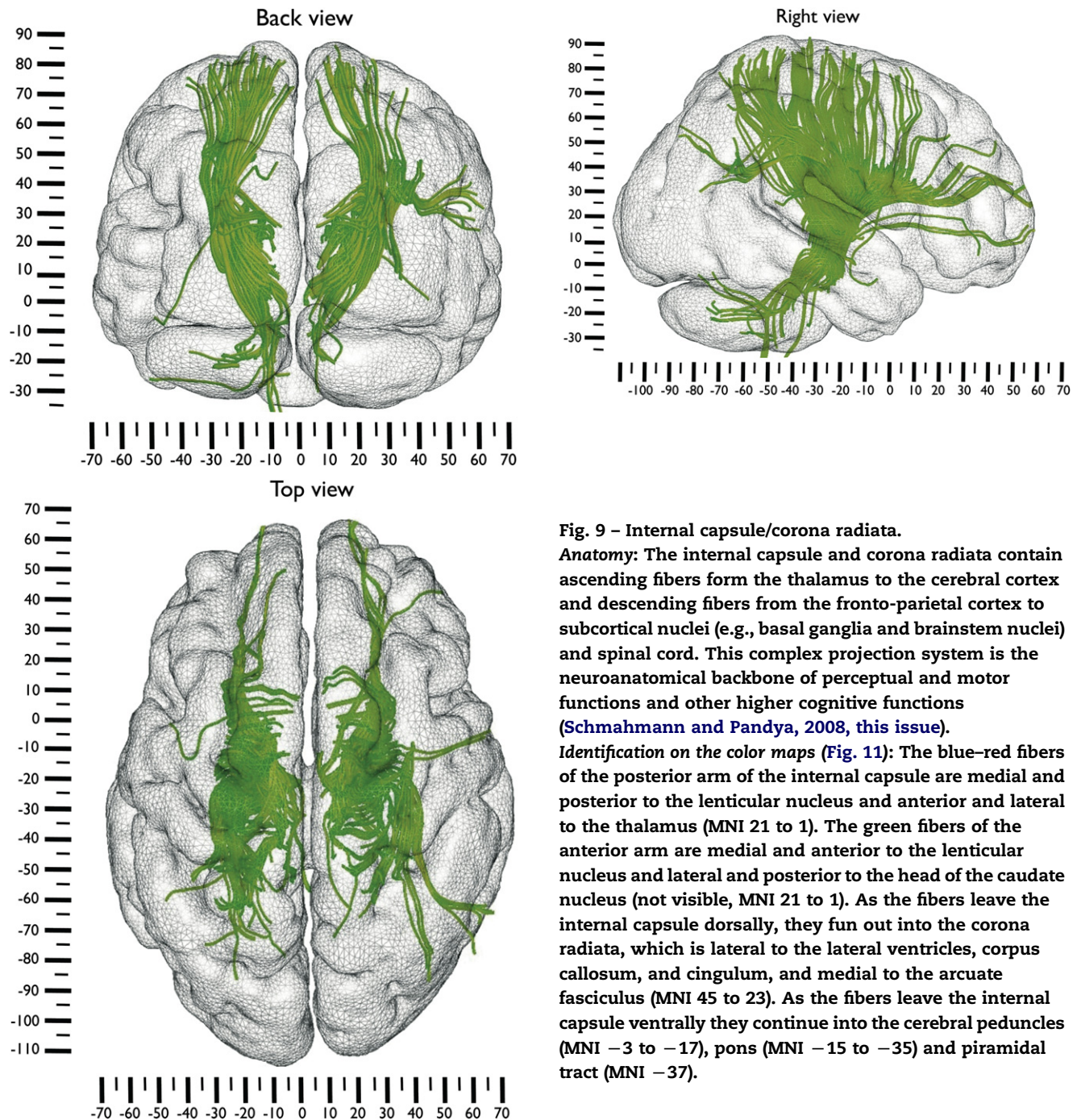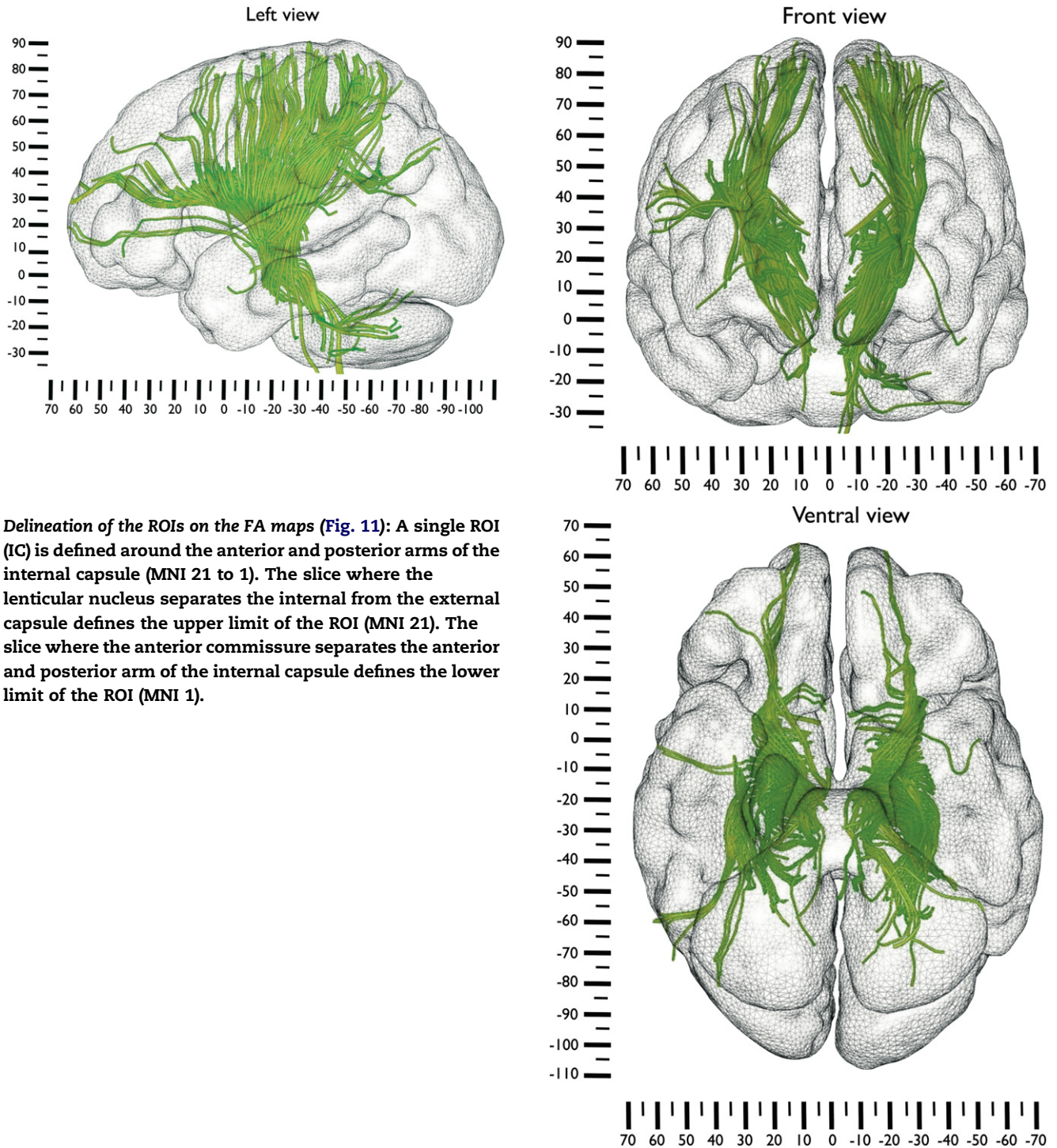
Fig. 9 – Internal capsule/corona radiata.

Anatomy: The internal capsule and corona radiata contain ascending fibers form the thalamus to the cerebral cortex and descending fibers from the fronto-parietal cortex to subcortical nuclei (e.g., basal ganglia and brainstem nuclei) and spinal cord. This complex projection system is the neuroanatomical backbone of perceptual and motor functions and other higher cognitive functions (Schmahmann and Pandya, 2008, this issue).

Identification on the color maps (Fig. 11): The blue–red fibers of the posterior arm of the internal capsule are medial and posterior to the lenticular nucleus and anterior and lateral to the thalamus (MNI 21 to 1). The green fibers of the anterior arm are medial and anterior to the lenticular nucleus and lateral and posterior to the head of the caudate nucleus (not visible, MNI 21 to 1). As the fibers leave the internal capsule dorsally, they fun out into the corona radiata, which is lateral to the lateral ventricles, corpus callosum, and cingulum, and medial to the arcuate fasciculus (MNI 45 to 23). As the fibers leave the internal capsule ventrally they continue into the cerebral peduncles (MNI −3 to −17), pons (MNI −15 to −35) and piramidal tract (MNI −37).

Left view

Front view

Ventral view

Delineation of the ROIs on the FA maps (Fig. 11): **A single ROI (IC) is defined around the anterior and posterior arms of the internal capsule (MNI 21 to 1). The slice where the lenticular nucleus separates the internal from the external capsule defines the upper limit of the ROI (MNI 21). The slice where the anterior commissure separates the anterior and posterior arm of the internal capsule defines the lower limit of the ROI (MNI 1).**
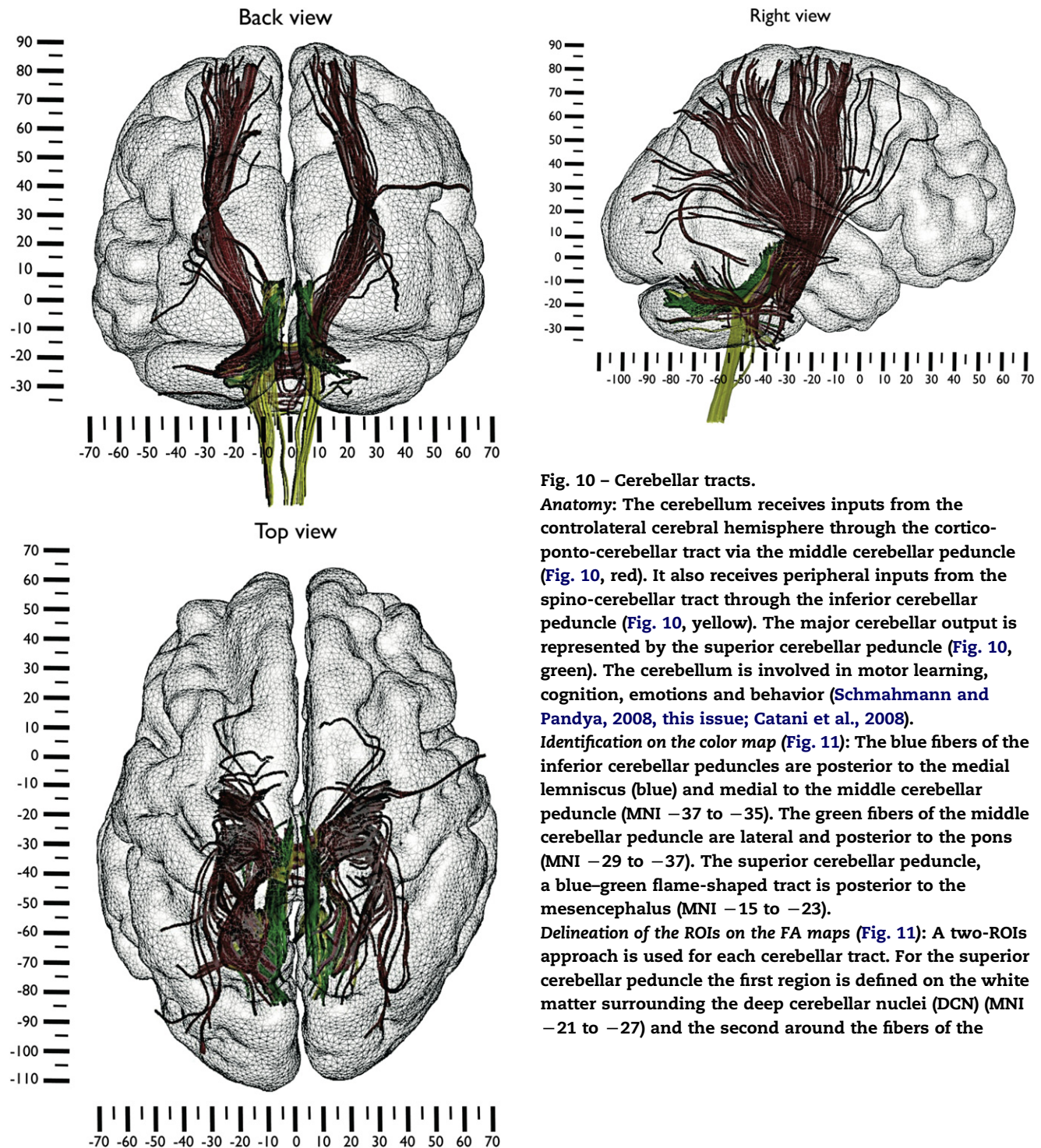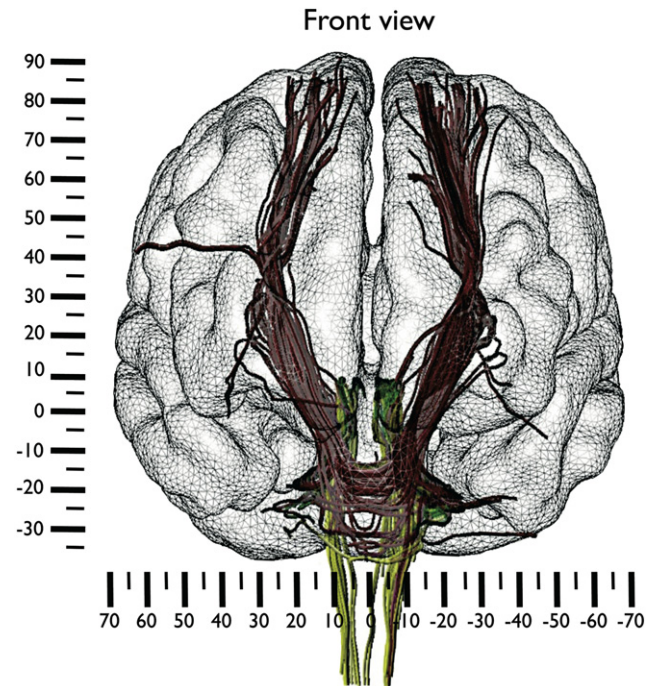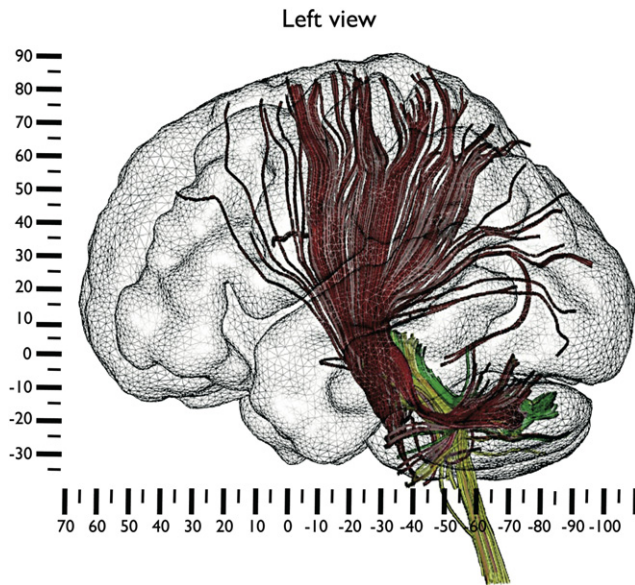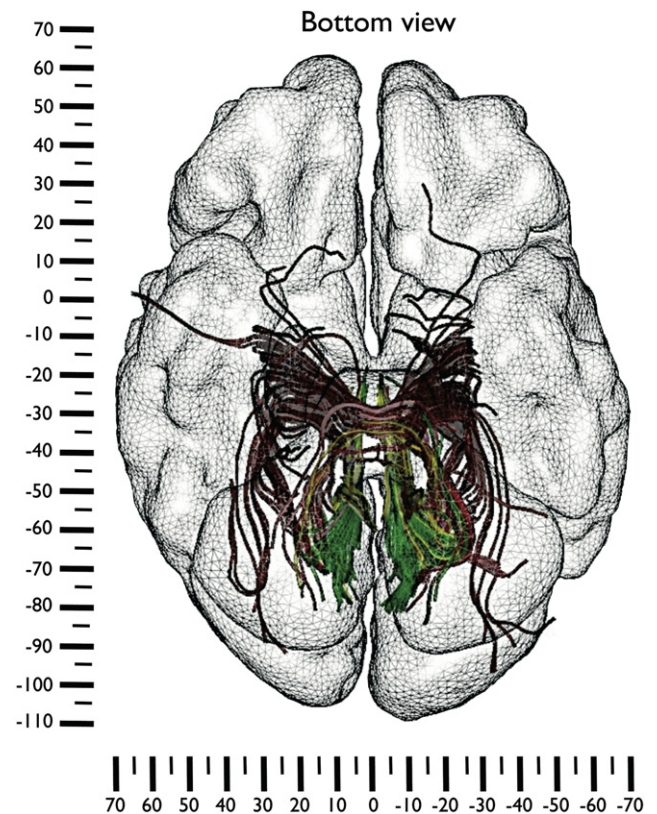
Fig. 10 – Cerebellar tracts.

Anatomy: The cerebellum receives inputs from the controlateral cerebral hemisphere through the cortico-ponto-cerebellar tract via the middle cerebellar peduncle (Fig. 10, red). It also receives peripheral inputs from the spino-cerebellar tract through the inferior cerebellar peduncle (Fig. 10, yellow). The major cerebellar output is represented by the superior cerebellar peduncle (Fig. 10, green). The cerebellum is involved in motor learning, cognition, emotions and behavior (Schmahmann and Pandya, 2008, this issue; Catani et al., 2008).

Identification on the color map (Fig. 11): The blue fibers of the inferior cerebellar peduncles are posterior to the medial lemniscus (blue) and medial to the middle cerebellar peduncle (MNI −37 to −35). The green fibers of the middle cerebellar peduncle are lateral and posterior to the pons (MNI −29 to −37). The superior cerebellar peduncle, a blue–green flame-shaped tract is posterior to the mesencephalus (MNI −15 to −23).

Delineation of the ROIs on the FA maps (Fig. 11): A two-ROIs approach is used for each cerebellar tract. For the superior cerebellar peduncle the first region is defined on the white matter surrounding the deep cerebellar nuclei (DCN) (MNI −21 to −27) and the second around the fibers of the

Left view

Front view

superior cerebellar peduncle (SCP) as they leave the cerebellum and enter the brainstem (MNI −15). For the cortico-ponto-cerebellar tract the first region is defined around the cerebral peduncle (MCP) of one side (MNI −11) and the second around the middle cerebellar peduncle on the other side (MNI −29 to −37). Finally for the inferior cerebellar peduncle the first region is defined around the deep cerebellar nuclei (the same region used for the superior cerebellar peduncle) and the second is defined around the fibers of the inferior cerebellar peduncle (ICP) (MNI −37).

Bottom view

ROIs legend

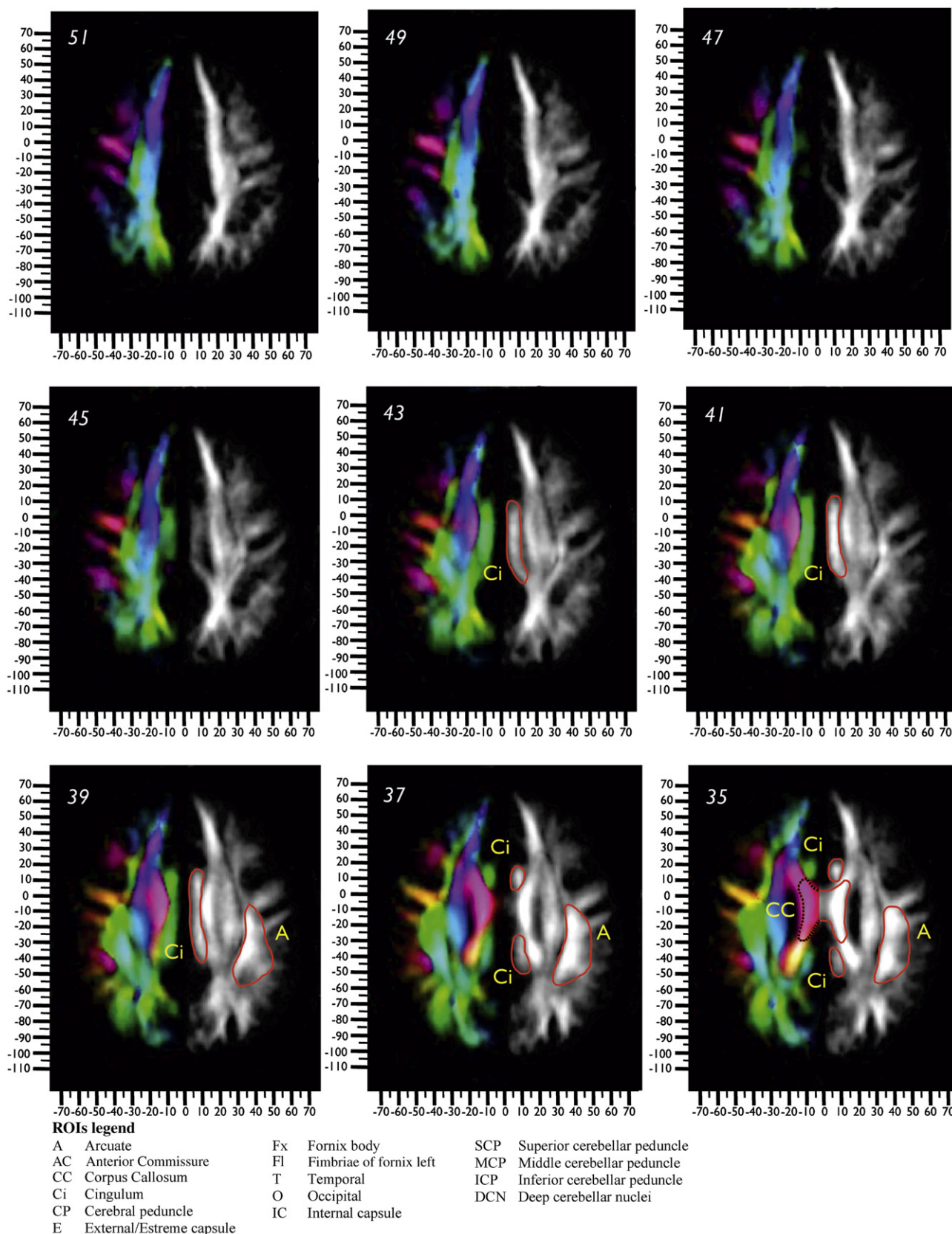|					
A	Arcuate	Fx	Fornix body	SCP	Superior cerebellar peduncle
AC	Anterior Commissure	Fl	Fimbriae of fornix left	MCP	Middle cerebellar peduncle
CC	Corpus Callosum	T	Temporal	ICP	Inferior cerebellar peduncle
Ci	Cingulum	O	Occipital	DCN	Deep cerebellar nuclei
CP	Cerebral peduncle	IC	Internal capsule		
E	External/Estreme capsule				

Fig. 11 – Diffusion tensor image template of an average data set and delineation of ROIs. The FA maps on the right provide information about the general anatomy of the major association, commissural and projection white matter tracts. The color maps on the left provide additional information on the local orientation of the tracts, where red color indicates a latero-lateral direction (left to right and right to left), green color an anterior–posterior direction (and vice versa), and blue color a dorsal–ventral direction (and vice versa). Other colors indicate intermediate directions.

ROIs legend

A	Arcuate	Fx	Fornix body	SCP	Superior cerebellar peduncle
AC	Anterior Commissure	Fl	Fimbriae of fornix left	MCP	Middle cerebellar peduncle
CC	Corpus Callosum	T	Temporal	ICP	Inferior cerebellar peduncle
Ci	Cingulum	O	Occipital	DCN	Deep cerebellar nuclei
CP	Cerebral peduncle	IC	Internal capsule		
E	External/Estreme capsule				

Fig. 11 – *Continued*

ROIs legend

A	Arcuate	Fx	Fornix body	SCP	Superior cerebellar peduncle
AC	Anterior Commissure	Fl	Fimbriae of fornix left	MCP	Middle cerebellar peduncle
CC	Corpus Callosum	T	Temporal	ICP	Inferior cerebellar peduncle
Ci	Cingulum	O	Occipital	DCN	Deep cerebellar nuclei
CP	Cerebral peduncle	IC	Internal capsule		
E	External/Estreme capsule				

Fig. 11 – *Continued*

ROIs legend

A	Arcuate	Fx	Fornix body	SCP	Superior cerebellar peduncle
AC	Anterior Commissure	Fl	Fimbriae of fornix left	MCP	Middle cerebellar peduncle
CC	Corpus Callosum	T	Temporal	ICP	Inferior cerebellar peduncle
Ci	Cingulum	O	Occipital	DCN	Deep cerebellar nuclei
CP	Cerebral peduncle	IC	Internal capsule		
E	External/Estreme capsule				

Fig. 11 – *Continued*

ROIs legend

A	Arcuate	Fx	Fornix body	SCP	Superior cerebellar peduncle
AC	Anterior Commissure	Fl	Fimbriae of fornix left	MCP	Middle cerebellar peduncle
CC	Corpus Callosum	T	Temporal	ICP	Inferior cerebellar peduncle
Ci	Cingulum	O	Occipital	DCN	Deep cerebellar nuclei
CP	Cerebral peduncle	IC	Internal capsule		
E	External/Estreme capsule				

Fig. 11 – *Continued*

of this second approach is that the method requires a priori anatomical knowledge to identify the course of white matter pathways and delineate ROIs on DTI images. Here, we provide a tool to teach tractography-derived white matter anatomy and to perform virtual in vivo dissections of the major tracts of the human brain. First, we have created a 3D tractography atlas of the associative, commissural and projection pathways in a standardized system of coordinates (Montreal Neurological Institute, MNI space) (Figs. 1–10). The atlas, together with the description of each tract in the figure legends, can be used as anatomical reference. Second, we provide some guidelines for the identification of the pathways in the color maps and show how to delineate ROIs on axial fractional anisotropy (FA) images from an average data set (Fig. 11). We hope that the atlas and the template for ROIs will be used as a tool for teaching and guiding virtual brain dissections in single cases and case–control studies.

2.   Methods

2.1.   DTI data set acquisition, processing, and averaging

Twelve right-handed male subjects (34.3 ± 5.7 years old) gave written consent to participate in the study, which was approved by the local ethics committee at the Service Hospitalier Frédéric Joliot, Orsay. MRI data were acquired using echo-planar imaging at 1.5 T (General Electric Healthcare Signa) with a standard head coil for signal reception. High resolution T1-weighted anatomical images were acquired (gradient-echo sequence, repetition time 9.9 ms, echo time 2 ms, matrix 256×192, field of view 24 cm, slice thickness 1.2 mm). DTI axial slices were obtained using the following parameters: repetition time 19 s; echo time 93 ms; flip angle 90°; voxel size $1.88 \times 1.88 \times 2$ mm, 200 independent directions, b-value 3000 s/mm^2. Raw diffusion-weighted data were corrected for geometric distortion secondary to eddy currents using a registration technique based upon the geometric model of distortions (Mangin et al., 2002). Two representative data sets were used to perform virtual dissections and create a 3D atlas of the major white matter tracts in the MNI space (Fig. 1–10). The 12 data sets were spatially normalized and averaged using a method similar to the method previously described by Jones et al. (2002). Briefly, the method includes the following steps: (i) registration of individual T1 images with the diffusion tensor data sets; (ii) normalization of the registered T1 using both linear and non-linear parameters; (iii) normalization of the diffusion tensor data sets using the deformation parameters derived from (ii); (iv) averaging of the normalized diffusion tensor data set. For the registration we used BRAINVISA 3.0.2 (http://brainvisa.info), which allows reorientation of each tensor correctly along the AC/PC plan. For the normalization we used statistical parametric mapping software (SPM5, Welcome Department of Cognitive Neurology, Institute of Neurology, London, UK, http://www.fil.ion.ucl.ac.uk/) and MATLAB version 7 (The Mathworks, Inc., MA, USA). Images were spatially normalized to the standard T1 template provided in SPM5. The 3D tractography reconstructions of each tract were registered in the MNI space and visualized within a glass brain using BRAINVISA 3.0.2.

2.2.   DTI template for the delineation of the ROIs

We combined color and FA diffusion tensor images to create a split-half template from an average data set. The axial diffusion images are presented in Fig. 11. The FA maps of the right hemisphere provide information about the general anatomy of the principal white matter tracts. The color maps of the left hemisphere provide additional information on the local orientation of the tracts, where red color indicates a latero-lateral direction (left to right and right to left), green color an anterior–posterior direction (and vice versa), and blue color a dorsal–ventral direction (and vice versa). Other colors indicate intermediate orientations. ROIs are defined on the axial FA images and were used as starting regions for tracking. Unlike other methods that use cortical masks as starting regions, the approach adopted here defines ROIs around areas of white matter that represent "obligatory passages" along the course of each tract. These obligatory passages represent brain regions that all fibres of each tract must pass through in order to reach their cortical or subcortical endstations (Catani et al., 2002). Hence, the use of obligatory passages as starting seed points for tracking allows to visualize all fibers of a single tract without constraining its cortical projections, which may vary from subject to subject. For example, all projection fibers from the thalamus to the cerebral hemisphere or from the cerebral hemisphere to spinal cord pass through the internal capsule to reach their endstations; hence the internal capsule represents the obligatory passage for this thalamo-cortico and cortico-spinal projection system. If the ROI representing an obligatory passage contains only fibres of the tract of interest, a single (one) ROI approach is used (i.e., all fibres passing through the ROI are displayed and considered as belonging to a single tract). A one-ROI approach is used for the arcuate fasciculus, cingulum, corpus callosum, anterior commissure and fornix. Other tracts share their obligatory passages with one or more tracts. In this case a two-ROIs approach is used where a second ROI is defined, such that it contains at least a section of the desired fasciculus but does not contain any fibers of the undesired fasciculi that pass through the first ROI (Conturo et al., 1999). Two-ROIs approach is used for the cerebellar tracts and the uncinate, inferior longitudinal and inferior fronto-occipito fasciculi. A second ROI can also be used to exclude undesired streamlines (i.e., display all fibers passing though the first ROI but not the second ROI). The inter-subjects reliability of this method was calculated among 10 operators in relation to an experienced tractographer (MC). All operators dissected ten tracts from a single dataset and measured diffusivity indexes from the dissected tracts. Pearson's correlation between each operator and the expert tractographer was calculated. A high inter-subject reliability was found for the volume of the ROIs (mean $r=.998$, SD$=.001$), number of streamlines (mean $r=.998$, SD$=.001$), volume of the tracts (mean $r=.998$, SD$=.0009$), length of the tracts (mean $r=.994$, SD$=.008$) and tract-specific FA measurements (mean $r=.958$, SD$=.053$).

REFERENCES

Basser PJ, Pajevic S, Pierpaoli C, Duda J, and Aldroubi A. In vivo fiber tractography using DT-MRI data. *Magnetic Resonance in Medicine*, 44: 625–632, 2000.

Balsamo M, Trojano L, Giamundo A, and Grossi D. Left hand tactile agnosia after posterior callosal lesion. *Cortex*, 44: 1030–1036, 2008.

Catani M. Diffusion tensor magnetic resonance imaging tractography in cognitive disorders. *Current Opinion in Neurology*, 19: 599–606, 2006.

Catani M. From hodology to function. *Brain*, 130: 602–605, 2007.

Catani M, Jones DK, Donato R, and ffytche DH. Occipito-temporal connections in the human brain. *Brain*, 126: 2093–2107, 2003.

Catani M, Jones DK, and ffytche DH. Perisylvian language networks of the human brain. *Annals of Neurology*, 57: 8–16, 2005.

Catani M, Allin M, Husain M, Pugliese L, Mesulam M, Murray R, et al. Symmetries in human brain language pathways predict verbal recall. *Proceedings of the National Academy of Sciences of the United States of America*, 104: 17163–17168, 2007.

Catani M, Jones D, Daly E, Deeley Q, Embiricos N, Pugliese L, et al. Altered cerebellar feedback projections in Asperger syndrome. *Neuroimage*, 41: 1184–1191, 2008.

Catani M, Howard RJ, Pajevic S, and Jones DK. Virtual in vivo interactive dissection of white matter fasciculi in the human brain. *Neuroimage*, 17: 77–94, 2002.

Concha L, Beaulieu C, and Gross DW. Bilateral limbic diffusion abnormalities in unilateral temporal lobe epilepsy. *Annals of Neurology*, 57: 188–196, 2005.

Conturo TE, Lori NF, Cull TS, Akbudak E, Snyder AZ, Shimony JS, et al. Tracking neuronal fiber pathways in the living human brain. *Proceedings of the National Academy of Sciences of the United States of America*, 96: 10422–10427, 1999.

Catani M and Mesulam M. What is a disconnection syndrome? *Cortex*, 44: 911–913, 2008a.

Catani M and Mesulam M. The arcuate fasciculus and the disconnection theme in language and aphasia: history and current state. *Cortex*, 44: 953–961, 2008b.

Doricchi F, de Thiebaut de Schotten M, Tomaiuolo F, and Bartolomeo P. White matter (dis)connections and gray matter (dys)functions in visual neglect: Gaining insights into the brain networks of spatial awareness. *Cortex*, 44: 983–995, 2008.

Doron KW and Gazzaniga MS. Neuroimaging techniques offer new perspectives on callosal transfer and interhemispheric communication. *Cortex*, 44: 1023–1029, 2008.

Epelbaum S, Pinel P, Gaillard R, Delmaire C, Perrin M, and Dupont S, et al. Pure alexia as a disconnection syndrome: New diffusion imaging evidence for an old concept. *Cortex*, 44: 962–974, 2008.

Fox CJ, Iaria G, and Barton JJS. Disconnection in prosopagnosia and face processing. *Cortex*, 44: 996–1009, 2008.

ffytche DH. The hodology of hallucinations. *Cortex*, 44: 1067–1083, 2008.

ffytche DH and Catani M. Beyond localization: from hodology to function. *Philosophical Transactions of the Royal Society of London B Biological Sciences*, 360: 767–779, 2005.

Gaffan D and Wilson CRE. Medial temporal and prefrontal function: Recent behavioural disconnection studies in the macaque monkey. *Cortex*, 44: 928–935, 2008.

Glickstein M and Berlucchi G. Classical disconnection studies of the corpus callosum. *Cortex*, 44: 914–927, 2008.

Heilmann KM and Watson RT. Disconnectional apraxia. *Cortex*, 44: 975–982, 2008.

Jones DK. Determining and visualizing uncertainty in estimates of fiber orientation from diffusion tensor MRI. *Magnetic Resonance in Medicine*, 49: 7–12, 2003.

Jones DK. Studying connections in the living human brain with diffusion MRI. *Cortex*, 44: 936–952, 2008.

Jones DK, Griffin LD, Alexander DC, Catani M, Horsfield MA, Howard R, et al. Spatial normalization and averaging of diffusion tensor MRI data sets. *Neuroimage*, 17: 592–617, 2002.

Lawes IN, Barrick TR, Murugam V, Spierings N, Evans DR, Song M, et al. Atlas-based segmentation of white matter tracts of the human brain using diffusion tensor tractography and comparison with classical dissection. *Neuroimage*, 39: 62–79, 2008.

Mangin JF, Poupon C, Clark C, Le Bihan D, and Bloch I. Distortion correction and robust tensor estimation for MR diffusion imaging. *Med Image Anal*, 6: 191–198, 2002.

Mori S, Kaufmann WE, Pearlson GD, Crain BJ, Stieltjes B, Solaiyappan M, et al. In vivo visualization of human neural pathways by magnetic resonance imaging. *Annals of Neurology*, 47: 412–414, 2000.

Rudrauf D, Mehta S, and Grabowski T. Disconnection's renaissance takes shape: Formal incorporation in group-level lesion studies. *Cortex*, 44: 1084–1096, 2008.

Ross ED. Sensory-specific amnesia and hypoemotionality in humans and monkeys: Gateway for developing a hodology of memory. *Cortex*, 44: 1010–1022, 2008.

Schmahmann J and Pandya DN. Disconnection syndromes of basal ganglia, thalamus, and cerebrocerebellar systems. *Cortex*, 44: 1037–1066, 2008.

Thiebaut de Schotten M, Kinkingnéhun S, Delmaire C, Lehéricy S, Duffau H, and Thivard L, et al. Visualization of disconnection syndromes in humans. *Cortex*, 44: 1097–1103, 2008.